

2MASS 22344161+4041387AB: A Wide, Young, Accreting, Low-mass Binary in the LkH α 233 Group¹

K. N. Allers², Michael C. Liu³

Institute for Astronomy, University of Hawaii, 2680 Woodlawn Drive, Honolulu, HI 96822

Evgenya Shkolnik⁴

*Department of Terrestrial Magnetism, Carnegie Institute of Washington, 5241 Broad
Branch Road, NW, Washington, DC 20015*

Michael C. Cushing², Trent J. Dupuy, Geoffrey S. Mathews²

Institute for Astronomy, University of Hawaii, 2680 Woodlawn Drive, Honolulu, HI 96822

I. Neill Reid

Space Telescope Science Institute, 3700 San Martin Drive, Baltimore, MD 21218

Kelle L. Cruz⁵

Department of Astronomy, California Institute of Technology, Pasadena, CA 91125

W. D. Vacca²

SOFIA-USRA, NASA Ames Research Center, MS N211-3, Moffett Field, CA 94035

ABSTRACT

We report the discovery of a young, 0.16'' binary, 2M2234+4041AB, found as the result of a Keck laser guide star adaptive optics imaging survey of young field ultracool dwarfs. Spatially resolved near-infrared photometry and spectroscopy indicate that the luminosity and temperature ratios of the system are near unity. From optical and near-infrared spectroscopy, we determine a composite spectral type of M6 for the system. Gravity-sensitive spectral features in the spectra of 2M2234+4041AB are best matched to those of young objects (~ 1 Myr old). A comparison of the T_{eff} and age of 2M2234+4041AB to evolutionary models indicates the mass of each component is $0.10^{+0.075}_{-0.04} M_{\odot}$. Emission lines of H α in the composite optical spectrum of the system and Br γ in spatially resolved near-IR spectra of the two components indicate that the system is actively accreting. Both components of the system have IR excesses, indicating that they

both harbor circumstellar disks. Though 2M2234+4041AB was originally identified as a young field dwarf, it lies $1.5'$ from the well-studied Herbig Ae/Be star, LkH α 233. The distance to LkH α 233 is typically assumed to be 880 pc. It is unlikely 2M2234+4041AB could be this distant, as it would then be more luminous than any known Taurus objects of similar spectral type. We re-evaluate the distance to the LkH α 233 group and find a value of 325_{-50}^{+72} pc, based on the *Hipparcos* distance to a nearby B3-type group member (HD 213976). 2M2234+4041AB is the first low-mass star to be potentially associated with the LkH α 233 group. At a distance of 325 pc, its projected physical separation is 51 AU, making it one of a growing number of wide, low-mass binaries found in young star-forming regions.

Subject headings: stars: formation, stars: low-mass, stars: binaries: visual, infrared: stars

1. Introduction

The binary fractions, mass ratios and separations of very low-mass (VLM; $M_{\star} \lesssim 0.1 M_{\odot}$) binaries can provide critical tests to theories of VLM star and brown dwarf formation. In addition to the same mechanism that forms low-mass stars, there are a number of suggested processes for forming brown dwarfs (Whitworth et al. 2007). These include gravitational instabilities in massive circumstellar disks (e.g. Stamatellos & Whitworth 2008), turbulent or gravitationally enhanced fragmentation (e.g. Padoan & Nordlund 2004; Bonnell et al. 2008), ejection from protostellar embryos (e.g. Bate & Bonnell 2005; Clarke et al. 2001), and photoevaporation of protostellar cores (Whitworth & Zinnecker 2004). These various formation

¹Some of the data presented herein were obtained at the W.M. Keck Observatory, which is operated as a scientific partnership among the California Institute of Technology, the University of California and the National Aeronautics and Space Administration. The Observatory was made possible by the generous financial support of the W.M. Keck Foundation.

²Visiting Astronomer at the Infrared Telescope Facility, which is operated by the University of Hawaii under Cooperative Agreement no. NCC 5-538 with the National Aeronautics and Space Administration, Office of Space Science, Planetary Astronomy Program.

³Alfred P. Sloan Research Fellow

⁴Carnegie Fellow

⁵Spitzer Fellow

mechanisms proposed for brown dwarfs are expected to result in differing binary fractions, mass ratios, and separations.

To date, imaging surveys for VLM binaries have focused on field ($\gtrsim 1$ Gyr old) objects (e.g. Burgasser et al. 2006; Goldman et al. 2008; Reid et al. 2006; Siegler et al. 2005; Liu et al. in prep), and have found much lower binary fractions (7–15% reported by Burgasser et al. (2007); 20% if corrected for completeness (Allen 2007)) than found for solar-type field stars (44%, Duquennoy & Mayor 1991). The detected field VLM binaries also tend to be tightly bound and in nearly equal mass systems, whereas higher mass field binaries have a much wider range of separations and mass ratios. It is difficult, however, to robustly test models of brown dwarf formation with field binary statistics for a number of reasons. First, wide VLM binaries could be dynamically disrupted by the time the systems reach the age of the field population (Close et al. 2007). Additionally, the intrinsic faintness and large changes in luminosity with mass for field objects (e.g. Baraffe et al. 2003) mean that low-mass ratio systems were unlikely to be detected by existing high resolution imaging surveys. Lastly, the field population is comprised of objects that were formed in a variety of star-forming regions with varying initial conditions, so comparison to model calculations for brown dwarfs forming in a single molecular cloud may be inappropriate.

To provide a better test of brown dwarf and star formation models, one would like to compare the binary properties of young, VLM objects to model predictions. The statistics for young, low-mass binaries are still uncertain. Ahmic et al. (2007) combined their survey with results from Kraus et al. (2005, 2006) and Konopacky et al. (2007) and report a combined binary fraction of $7_{-3}^{+4}\%$ for 72 young, low-mass stars and brown dwarfs. This binary fraction is similar to the binary fraction for field VLM binaries (7–15%, Burgasser et al. 2007). However, because the nearest star-forming regions are ~ 125 pc away, only wide binaries can be detected by current imaging surveys. The Ahmic et al. (2007) binary fraction is valid only for young VLM binaries with separations greater than 8 AU, whereas field VLM binaries tend to have tighter separations (Burgasser et al. 2007). Thus, the actual young binary fraction would be significantly higher than the fraction found for field VLM binaries, if surveys for young and field VLM binaries reached the same physical separation limits. Young star-forming regions also show an interesting population of very wide separation ($\gtrsim 100$ AU), loosely bound VLM binaries (Béjar et al. 2008; Bouy et al. 2006; Close et al. 2007; Luhman 2004a). The fate of these wide binaries is unknown, as it is unlikely that they could survive ejection or dispersal from their natal clouds, given their low binding energies.

To probe the multiplicity properties of young VLM objects at tight separations and look for wide systems in the field that have not yet dissolved, we are carrying out a Keck laser guide star adaptive optics (LGS AO) survey to image young ($\lesssim 100$ Myr), field VLM

objects. This paper presents the first results of this program. This survey is a part of our larger, ongoing effort using LGS AO to study the multiplicity of VLM objects and determine their fundamental properties (e.g. Dupuy, Liu, & Ireland 2008; Liu, Dupuy, & Ireland 2008; Liu et al. 2006).

Young field objects are usually found in three ways: as companions to known young field stars (Rebolo et al. 1998), via association with known young moving groups (e.g. Gizis 2002), or serendipitously as a part of searches for older field dwarfs (e.g. Kirkpatrick et al. 2008). 2MASS J22344161+4041387 (hereinafter 2M2234+4041AB) was identified by Cruz et al. (2003) as a candidate young M6-type object. They classified the object as young on the basis of weak CaH (6750–7050 Å) and KI doublet (7665 and 7699 Å) absorption and strong H α emission seen in its low-resolution optical spectrum.

Using Keck LGS AO, we have discovered 2M2234+4041AB to be a binary system. In this paper, we present multi-wavelength imaging and spectroscopy used to determine the properties of 2M2234+4041AB.

2. Observations

2.1. Keck LGS AO/NIRC2 Imaging

We imaged 2M2234+4041AB on three epochs from 2006–2008 using the laser guide star adaptive optics (LGS AO) system (Wizinowich et al. 2006; van Dam et al. 2006) of the 10-meter Keck II Telescope on Mauna Kea, Hawaii. We used the facility IR camera NIRC2 with its narrow field-of-view camera, which produces a $10.2'' \times 10.2''$ field of view, and the Mauna Kea Observatories J , H , K_S and L' filters (Simons & Tokunaga 2002; Tokunaga, Simons & Vacca 2002). Images of 2M2234+4041AB are presented in Figure 1. Setup time for the telescope to slew to the science target and for the LGS AO system to be fully operational varied from 4–21 minutes on the observing runs. The LGS brightness was equivalent to a $V \approx 9.4 - 10.1$ mag star, as measured by the flux incident on the AO wavefront sensor. The LGS provided the wavefront reference source for AO correction, with the exception of tip-tilt motion. Tip-tilt aberrations and quasi-static changes in the image of the LGS as seen by the wavefront sensor were measured contemporaneously with a second, lower-bandwidth wavefront sensor monitoring 2M2234+4041AB itself ($R=16.8$; Monet et al. 2003). The sodium laser beam was pointed at the center of the NIRC2 field-of-view for all observations.

For the JHK_S filters, we obtained a series of dithered images, offsetting the telescope by a few arc-seconds. The resulting images were reduced in the standard fashion (dome flat-

fielded, median sky-subtracted, registered and stacked). The L' -band data were observed and reduced in a similar fashion, except that the flat fields were constructed from the science frames themselves and sky subtraction was done in a pairwise fashion using consecutive frames.

To measure the flux ratios and relative positions of the binary’s two components, we used an analytic model of the point spread function (PSF) as the sum of three elliptical gaussians. For the individual images obtained with each filter, we fitted for the flux ratio, separation, and position angle of the binary. The averages of the results were adopted as the final measurements and the standard deviations as the errors. The relative astrometry was corrected for instrumental optical distortion based on analysis by B. Cameron (priv. comm.) of images of a precisely machined pinhole grid located at the first focal plane of NIRC2. Since the binary separation and the imaging dither steps are relatively small, the effect of the distortion correction is minor.

In order to gauge the accuracy of our measurements, we created myriad artificial binary stars from images of single stars, chosen to have comparable Strehl and FWHM as the science data. For each filter, our fitting code was applied to artificial binaries with similar separations and flux ratios as 2M2234+4041AB over a range of PAs. These simulations showed that any systematic offsets in our fitting code are very small, well below the random errors, and that the random errors are accurate. In cases where the RMS measurement errors from the artificial binaries were larger than those from the 2M2234+4041AB measurements, we conservatively adopted the larger errors. The exception was the L' -band data, where the prominent first Airy ring seen in the images coincides with the separation of the binary. The results from the simulated L' -band binaries indicated a significant (1.5σ) shift in the astrometry, so this was applied to the raw measurements; the shift moves the L' -band astrometry into better agreement with the JHK_S results.

To convert the instrumental measurements of the binary’s separation and PA into celestial units, we used a weighted average of the calibration from Pravdo et al. (2006), with a pixel scale of 9.963 ± 0.011 mas/pixel and an orientation for the detector’s +y axis of $0.13 \pm 0.07^\circ$ east of north for NIRC2’s narrow camera optics. These values agree well with Keck Observatory’s notional calibrations as well as the 9.963 ± 0.005 mas/pixel and $0.13 \pm 0.02^\circ$ reported by Ghez et al. (2008). Table 1 presents our final Keck LGS imaging measurements.

2.2. IRTF/SpeX Near-IR Spectroscopy and L' Imaging

Near-IR spectroscopy of 2M2234+4041AB was obtained on 2008 June 25 (UT) using the SpeX spectrograph (Rayner et al. 2003) on the NASA Infrared Telescope Facility. The seeing recorded by the IRTF was $0.6''$. Six cycles of 180 second exposures were taken, nodding along the slit, for a total integration time of 36 minutes. The data were taken in SXD mode with a $0.3''$ slit (aligned with the parallactic angle) producing a $0.9\text{--}2.5\ \mu\text{m}$ spectrum with a resolution ($\lambda/\Delta\lambda$) of ~ 2000 . For telluric and flux correction, we observed a nearby A0V star, BD+39 4890 ($V=9.47$ mag) and obtained calibration frames (flats and arcs) prior to our observations of 2M2234+4041AB. For comparison to our spectrum of 2M2234+4041AB, we obtained SpeX spectra of USco CTIO 75 (M6, Ardila et al. 2000) on 2008 Jun 25 and spectra of Haro 6-32 (M5, Luhman 2004b), CFHT-BD-Tau 18 (M6, Guieu et al. 2006), and CFHT-BD-Tau 4 (M7, Luhman 2004b) on 2005 October 22. We used the same instrument setup as for our spectrum of 2M2234+4041AB, and obtained total integration times of 20 to 30 minutes per source. The spectra were reduced using Spextool (Cushing et al. 2004), the facility reduction pipeline, which includes a correction for telluric absorption following the method described in Vacca et al. (2003). Our SpeX spectra are presented in Figures 2 and 3.

To obtain integrated-light L' photometry (in the MKO system; Simons & Tokunaga 2002; Tokunaga, Simons & Vacca 2002) of 2M2234+4041AB (Table 2), we obtained images on 2008 September 24 (UT) using the SpeX guider camera. Conditions were photometric and the IRTF recorded a seeing of $\sim 0.6''$. We obtained a set of 10 nodded cycles of 300s exposures, nodding the telescope $7.7''$ in the north-south direction. We repeated this process for 2 additional positions. Between sets of 2M2234+4041AB images, we obtained images of the UKIRT faint standard FS2–27, using the same instrument and observing configuration. To flat field our images, we used the median of dome flats for the J, H, K, and HK filters (kindly provided to us by John Rayner). We subtracted each nodded pair, and median combined the resulting images at each position, for 6 final images of 2M2234+4041AB and 4 final images of FS2–27. We obtained aperture photometry for both 2M2234+4041AB and FS2–27 using an aperture radius of $1.2''$ (10 pixels). We calculated the mean and standard deviation of the fluxes measured at each position to determine our final photometry. We measured an integrated light flux of $L' = 10.52 \pm 0.06$ mag for 2M2234+4041AB.

2.3. Keck LGS AO/OSIRIS Spectroscopy

We obtained spatially resolved K -band spectroscopy of 2M2234+4041AB on 2008 June 30 (UT) using the OSIRIS integral field spectrograph (Larkin et al. 2003) and LGS AO

on the Keck-II telescope. We selected the 20 mas/pixel scale for our observations. We observed 2M2234+4041AB taking 8 dithered exposures of 120 seconds each, for a total of 16 minutes on source integration. The FWHM, as measured on the stacked 2D images of 2M2234+4041AB, was 68 ± 2 mas, thus the binary (158 mas separation) is well resolved. Immediately following our observations of 2M2234+4041AB, we obtained sky frames using the same dither pattern and integration time. To correct for telluric absorption, we obtained spectra of a nearby A0V star, HD 209932. The initial reduction from 2D images to 3D data cubes was accomplished using the OSIRIS data reduction pipeline (Krabbe et al. 2004). The individual spectra for each component were then extracted from the 3D data cubes by summing the flux in fixed apertures of 175×175 mas at each wavelength. The resulting spectra of each component were then median combined together. Telluric correction and flux calibration were performed using the observations of the A0 V standard and the technique described in Vacca et al. (2003). The resulting 1.96–2.38 μm spectra of 2M2234+4041A and B (Figure 4) have a resolution ($\lambda/\Delta\lambda$) of ~ 3500 , and median S/N of ~ 90 per pixel.

2.4. Keck HIRES Optical Spectroscopy

We acquired two optical spectra of 2M2234+4041AB on May 11 and August 12 of 2006 with the High Resolution Echelle Spectrometer (HIRES; Vogt et al. 1994) on the Keck I telescope. We used the 0.861" slit with HIRES to give a spectral resolution of $\lambda/\Delta\lambda \approx 58,000$. To maximize the throughput near the peak of a M dwarf spectral energy distribution, we used the GG475 filter with the red cross-disperser.

Each stellar exposure was bias-subtracted and flat-fielded for pixel-to-pixel sensitivity variations. After optimal extraction, the 1-D spectra were wavelength calibrated with a Th/Ar arc. Finally the spectra were divided by a flat-field response and corrected to the heliocentric rest frame. The final spectra were of moderate S/N reaching ~ 25 per pixel at 7000 Å.

We cross-correlated each of 7 orders between 7000 and 9000 Å of each stellar spectrum with a RV standard of similar spectral type using IRAF's⁶ *fxcor* routine (Fitzpatrick 1993). We excluded the Ca II infrared triplet (IRT)⁷ and regions of strong telluric absorption in

⁶IRAF (Image Reduction and Analysis Facility) is distributed by the National Optical Astronomy Observatories, which is operated by the Association of Universities for Research in Astronomy, Inc. (AURA) under cooperative agreement with the National Science Foundation.

⁷Since the target star exhibits Ca II emission that is not present in the RV standards, it was important to eliminate the IRT from the cross-correlation.

the cross-correlation. Radial velocities and relevant line equivalent widths measured from our HIRES data are listed in Table 4, and portions of our HIRES spectrum are displayed in Figures 5 and 6. Further details of HIRES data reduction and analysis are provided by Shkolnik, Liu & Reid (2009).

2.5. Proper Motion

To calculate a proper motion for 2M2234+4041AB, we used red and blue POSS-I⁸ images from the Digitized Sky Surveys⁹ and 12 i' and z' band images from the Tektronix 2048×2048 CCD camera (Tek) on the University of Hawaii 2.2-meter telescope kindly provided to us by Roy Gal. 2M2234+4041AB is well detected ($>30\sigma$) in all of the POSS-I and Tek images. The red and blue POSS-I images were taken on 1952 July 20 and have pixel scales of 1.7'' and 1.0'' per pixel respectively. The Tek images were taken on 2007 July 31 and have a pixelscale of 0.22'' per pixel. We used Source Extractor (Bertin & Arnouts 1996) to obtain the x and y positions of objects in individual images and used IRAF's xyxymatch and geomap routines (with 3rd order polynomial fits) to match detections within each epoch and spatially transform the detections to the image coordinate system of the POSS-I red image (for POSS-I epoch images) or the first Tek image (for all Tek images). The standard deviations of the fits found by geomap were $\sim 0.20''$ for the match of POSS-I red and blue images and $\sim 0.04''$ for the match of the Tek images. We then calculated the average x and y positions within each epoch, and used xyxymatch and geomap to match 107 sources and transform their POSS-I detected positions to the Tek image (x,y) coordinate system, giving us the Δx and Δy of 2M2234+4041AB. We then calculated the pixelscale and orientation of the Tek images using SCAMP (the Terapix astrometric software package), and converted Δx and Δy for 2M2234+4041AB to $\Delta\alpha$ and $\Delta\delta$. The standard deviations found by geomap for transforming the POSS-I detections to the Tek image coordinate system were 0.34'' in x and 0.27'' in y. The measured motion of 2M2234+4041AB from the POSS-I images to the Tek images is -58 ± 340 mas and 166 ± 270 mas respectively, resulting in a proper motion of -1 ± 6 and 3 ± 5 mas yr⁻¹ for $\mu_\alpha(\cos(\delta))$ and μ_δ respectively. Thus, 2M2234+4041AB shows no significant proper motion (Figure 7).

⁸The National Geographic Society - Palomar Observatory Sky Atlas (POSS-I) was made by the California Institute of Technology with grants from the National Geographic Society.

⁹The Digitized Sky Surveys were produced at the Space Telescope Science Institute under U.S. Government grant NAG W-2166. The images of these surveys are based on photographic data obtained using the Oschin Schmidt Telescope on Palomar Mountain and the UK Schmidt Telescope. The plates were processed into the present compressed digital form with the permission of these institutions.

3. Analysis

3.1. Spectral Type

We derive an optical spectral type by visually comparing the TiO and VO bands in our HIRES spectrum of 2M2234+4041AB to standard stars of known spectral types. For stars of spectral type \sim M5.5 or later, the 7140 Å TiO band weakens due to condensation onto grains whereas the VO band at 7300 Å strengthens with spectral type until M7, and then weakens for later types. This allows us to unambiguously classify 2M2234+4041AB as M6 with a conservative uncertainty of ± 1 subclass. The M6 optical spectral type we determine agrees with that of Cruz et al. (2003), who used low-resolution ($R \simeq 1400$) optical spectra.

We can also determine the spectral type of 2M2234+4041AB by comparing its SpeX near-IR spectrum to spectra of young objects in Taurus (Figure 2). We choose Taurus objects rather than field dwarfs for comparative spectral typing, as the spectral features of 2M2234+4041AB are consistent with a young age (see §3.3). Our near-IR spectrum of 2M2234+4041AB is a near perfect match to the spectrum of CFHT-BD-Tau 18, a young Taurus object with an optically determined spectral type of M6 (Guieu et al. 2006). The spectral type sensitive index ($\langle F_{\lambda=1.550-1.560} \rangle / \langle F_{\lambda=1.492-1.502} \rangle$) of Allers et al. (2007), which is calibrated for young and field stars with optical spectral types, suggests a spectral type of $M6.4 \pm 1$, in agreement with the spectral types we determine from visual inspection of optical and near-IR spectra. We assign a spectral type of $M6 \pm 1$ to both components of 2M2234+4041AB given the similarity of their near-IR colors (Table 1) and K-band spectra (Figure 4).

3.2. Extinction

To obtain intrinsic colors and magnitudes of 2M2234+4041AB we must determine the amount of dust attenuating the source. To compute the extinction, we compare the observed J–H color of 2M2234+4041AB to the colors of field and young objects. We choose to determine our extinction value using J–H for two reasons. First, of the available photometry of 2M2234+4041AB (Table 2), the J–H color is at the shortest wavelength and hence is the most sensitive to extinction, and the least likely to be contaminated by excess emission from a circumstellar disk. Second, the J–H color for mid to late M-type objects is insensitive to spectral type (Leggett et al. 2002), so uncertainties in the spectral type of 2M2234+4041AB do not affect our determination of extinction.

The mean 2MASS J–H color of M6 V objects from Dwarfarchives¹⁰ (Kirkpatrick et al. 1991; Kirkpatrick 1992; Kirkpatrick et al. 1995) is 0.58 mag with a standard deviation of 0.07 mag. The 2MASS J–H color of 2M2234+4041AB is 0.74 ± 0.03 mag. Dereddening the J–H color of 2M2234+4041AB (0.74 ± 0.03) to the field M6 V value, using $(A_J - A_H)/A_V = 0.1$ (values from ADPS¹¹), requires $A_V=1.6\pm 0.8$ mag. This may represent an upper limit on A_V , however, as young objects may have redder intrinsic colors than older field objects (Kirkpatrick et al. 2006). As a cross-check, we compiled 2MASS PSC photometry for 24 young M6 type objects in Upper Scorpius from Ardila et al. (2000) and Slesnick et al. (2006). At 5 Myr old, most of the gas and dust in the Upper Scorpius region has been dispersed by OB stars in the region. Thus Upper Scorpius objects should have very low dust extinction, and provide a good estimate of the intrinsic colors of young objects. The mean J–H color of the Upper Scorpius M6 objects is 0.69 mag, with a standard deviation of 0.07 mag, which implies $A_V=0.5\pm 0.8$ for 2M2234+4041AB, which is in agreement (to within the uncertainties) with the A_V we derive from comparison with field dwarf colors. Based on the A_V ’s and uncertainties from dereddening the J–H color of 2M2234+4041AB to field and young M6 objects, we adopt an extinction value of $A_V=1.1\pm 1.1$ mag.

3.3. Age

3.3.1. Lithium

Lithium is destroyed at core temperatures of $2 - 3 \times 10^6$ K. Such hot temperatures exist in the central regions of the lowest mass stars and high mass brown dwarfs ($\gtrsim 0.06 M_\odot$, Chabrier et al. 1996). The timescale for lithium depletion is dependent on mass, with higher mass stars burning their lithium more quickly than lower mass stars. Figure 5 shows lithium detected in the spectrum of 2M2234+4041AB, with an equivalent width of 0.83 ± 0.02 Å (the mean of the values listed in Table 4). Stauffer et al. (1998) found that Pleiades stars with spectral types earlier than M6.5 had depleted their lithium. Thus, for a spectral type of M6, the detection of lithium in 2M2234+4041AB places an upper limit on the age of $\lesssim 100$ Myr, based on the age of Pleiades (Meynet et al. 1993).

¹⁰<http://www.dwarfarchives.org>

¹¹The Asiago Database on Photometric Systems is available via <http://ulisse.pd.astro.it/Astro/ADPS/>

3.3.2. L' -band Excess

The detection of infrared emission in excess of that expected from the stellar photosphere is widely used as an indicator of circumstellar disks. Liu et al. (2003) found that objects with spectral types as late as M8 can exhibit excess emission in L' band. Figure 8 shows the $K_S - L'$ colors for 2M2234+4041A and B compared to the colors of field dwarfs (Leggett et al. 2002; Reid & Cruz 2002; Leggett et al. 2003). The dereddened $K_S - L'$ colors of 2M2234+4041A and B are 0.96 ± 0.06 mag and 0.78 ± 0.07 mag, whereas the average $K_S - L'$ color of M5–M7 type field dwarfs is 0.45 mag. Thus, 2M2234+4041A and B have $K_S - L'$ excesses detected at the 8 and 5 σ levels, respectively, and likely possess circumstellar disks. Half of primordial disks around stars dissipate by an age ~ 3 Myr and all have dissipated by ~ 6 Myr (Haisch et al. 2001). There is some evidence that primordial disks around brown dwarfs might be slightly longer-lived than disks around stars (e.g. Riaz & Gizis 2008), so it is difficult to place an upper limit on the age of 2M2234+4041AB based solely on the presence of its circumstellar disk.

It is important to note that while the absolute value of $K_S - L'$ for 2M2234+4041A and B has an uncertainty of 0.06–0.07 mag, the uncertainty in their *relative* $K_S - L'$ colors is smaller (0.04 mag), so the difference in the $K_S - L'$ colors of the two components is well detected ($\Delta K_S - L' = 0.18 \pm 0.04$ mag). The presence of circumstellar disks in both components of a wide, low-mass binary system is interesting, as such systems are rare (e.g. Allers et al. 2007). Given that 2M2234+4041A and B have nearly identical spectral types and J, H, K_S brightnesses and are presumably co-eval, the difference in their excess is particularly compelling, as it implies that the physical structures of their disks are different. Models of circumstellar disks (e.g. D'Alessio et al. 2006; Dullemond, Dominik & Natta 2001) indicate that differences in the radius of an inner disk hole, the height of the disk rim, the accretion rate, or the inclination of disk could explain the relative $K_S - L'$ colors of 2M2234+4041A and B. Unfortunately, with only $K_S - L'$ colors, we can not distinguish between these scenarios.

3.3.3. Accretion Indicators

Young, low-mass objects often show spectroscopic signatures of accretion from circumstellar disks. Atomic hydrogen lines, specifically $H\alpha$ emission, are commonly used to measure accretion rates. Table 4 lists the $H\alpha$ equivalent widths (EWs) and 10% widths measured in our HIRES spectra of 2M2234+4041AB. White & Basri (2003) found that non-accreting stars and brown dwarfs can have strong $H\alpha$ emission (EWs of -3 to -36 Å), presumably due to chromospheric activity, and proposed that M6–M7.5 type objects with $H\alpha$ EWs less than -40 Å are likely accreting. The $H\alpha$ EW we measure for 2M2234+4041AB in our 2006

May 11 spectrum is -52.7 \AA , well below the accretor limit, while the EW measured on 2006 Aug 12 (-39.2 \AA) is just above the limit. Both of our $\text{H}\alpha$ EW measurements, however, meet the accretor criterion of Barrado y Navascués & Martín (2003).

White & Basri (2003) proposed a more reliable determination of accretion, the 10% width of $\text{H}\alpha$ emission, which if greater than 270 km s^{-1} is indicative of accretion. The $\text{H}\alpha$ 10% widths we measure for 2M2234+4041AB (314 and 298 km s^{-1}) are above the 10% width requirement of White & Basri (2003) and well above the revised 200 km s^{-1} $\text{H}\alpha$ 10% width cutoff for very low-mass stars and brown dwarfs adopted by Mohanty et al. (2005). Thus 2M2234+4041AB is actively accreting. Following the procedure of Natta et al. (2004), we calculate a mass accretion rate of $1.2 \times 10^{-10} M_{\odot} \text{ yr}^{-1}$ from the average of our measured $\text{H}\alpha$ 10% widths in Table 4. The accretion rate we measure for 2M2234+4041AB is in good agreement with values for young M6 type objects in Taurus and Chamaeleon I determined by modeling the $\text{H}\alpha$ line emission profile (Muzerolle et al. 2005). Mohanty et al. (2005) found that the fraction of accreting low-mass stars and brown dwarfs drops significantly for ages greater than 5 Myr. Thus, the strong $\text{H}\alpha$ emission seen in the spectrum of 2M2234+4041AB implies that it is probably younger than 5 Myr.

The accretion rate we calculate from the $\text{H}\alpha$ equivalent width is measured from the *composite* HIRES spectra of 2M2234+4041AB. The OSIRIS K-band spectra of both 2M2234+4041A and B show $\text{Br}\gamma$ emission (Figure 4). Muzerolle et al. (1998) found that the luminosity of $\text{Br}\gamma$ line emission is well-correlated with the total accretion luminosity (determined from U-band or blue continuum emission) for late-K and early-M spectral type classical T Tauri stars. The relation between $\text{Br}\gamma$ and accretion luminosities was subsequently extended to higher and lower mass by Calvet et al. (2004) and Natta et al. (2006).

To measure the $\text{Br}\gamma$ luminosities for 2M2234+4041A and B, we flux calibrate our OSIRIS spectra using the Ks-band magnitude of each component, and then fit gaussians to the $\text{Br}\gamma$ line emission. We measure $\text{Br}\gamma$ equivalent widths of $-3.0 \pm 0.3 \text{ \AA}$ and $-2.5 \pm 0.3 \text{ \AA}$ and calculate $\log(L_{\text{Br}\gamma}/L_{\odot})$ of -5.20 ± 0.04 and -5.82 ± 0.05 for 2M2234+4041A and B respectively, assuming a distance of $325_{-50}^{+72} \text{ pc}$ to 2M2234+4041AB (see §3.4). The uncertainties are determined from the formal errors of the gaussian fit and do not include distance uncertainties. Using the relation between accretion luminosity and $\text{Br}\gamma$ luminosity from Muzerolle et al. (1998), we calculate accretion luminosities, $\log(L_{\text{acc}}/L_{\odot})$, of -2.1 ± 1.3 and -2.3 ± 1.3 for 2M2234+4041A and B. Assuming a mass of $0.1 M_{\odot}$ (§3.5) and a radius of $0.982 R_{\odot}$ (appropriate for a 1 Myr old, $0.1 M_{\odot}$ object (Baraffe et al. 1998)), we calculate accretion rates (from $\dot{M}_{\text{acc}} = L_{\text{acc}} R_{*} / (GM_{*})$) of 2.4 and $1.8 \times 10^{-9} M_{\odot} \text{ yr}^{-1}$ for 2M2234+4041A and B respectively. The accretion rates we measure from $\text{Br}\gamma$ are larger than the accretion rate we calculate from $\text{H}\alpha$, but given the large uncertainties in the $\text{Br}\gamma$ accretion luminosities and

the distance to the source, this is not unexpected. The accretion rates we measure from $\text{Br}\gamma$ and $\text{H}\alpha$ are consistent with values of \dot{M} for sources of similar mass (Muzerolle et al. 2005), and indicate that both components of 2M2234+4041AB are young and actively accreting.

3.3.4. Gravity Sensitive Spectral Features

To further constrain the age of 2M2234+4041AB we examine the gravity (age) sensitive absorption lines of K I and Na I (Allers et al. 2007; McGovern et al. 2004; Gorlova et al. 2003) in the SpeX J-band spectrum of 2M2234+4041AB. For comparison to the 2M2234+4041AB spectrum, we selected objects with ages determined by their membership in: the Taurus star-forming region (~ 1 Myr, Luhman et al. 2003a), the Upper Scorpius OB association (~ 5 Myr, Preibisch et al. 2002), the TW Hydra moving group (~ 10 Myr, Webb et al. 1999), and the general field dwarf population ($\gtrsim 1$ Gyr). We chose objects with optical spectral types of M6 (if available), so that we are comparing only the age sensitivity of spectral features. In Figure 3, we compare the SpeX spectrum of 2M2234+4041AB to SpeX spectra we obtained of CFHT-BD-Tau 18 (Taurus M6, Guieu et al. 2006), USco CTIO 75 (Upper Scorpius M6, Ardila et al. 2000), as well as a SpeX spectrum of TWA8B (TW Hydra M5, Webb et al. 1999) given to us by Casey Deen (*priv. comm.*), and a spectrum of Gl406, a field M6 from Cushing et al. (2005). In Figure 3, one can clearly see the increase in K I and Na I line strengths with age. The line strengths in 2M2234+4041AB are noticeably weaker than the field, TW Hydra, and Upper Scorpius objects, indicating an age for 2M2234+4041AB of less than 5 Myr. The K I and Na I line strengths (and the entire spectrum) of 2M2234+4041AB are best matched by CFHT-BD-Tau 18, implying an age of ~ 1 Myr for 2M2234+4041AB. The K I 7700Å line in the composite HIRES spectrum is also very weak and indicative of a young age (Shkolnik, Liu & Reid 2009). Our resolved OSIRIS K-band spectra of 2M2234+4041A and B have $2.2 \mu\text{m}$ Na I line strengths similar to a Taurus M6 (Figure 4), further indicating that both components of 2M2234+4041AB are young.

3.4. Distance

The distance to 2M2234+4041AB is the critical parameter for determining the physical separation of the system, as well as its luminosity and mass. Assuming 2M2234+4041AB is of similar age as objects in Taurus (§3.3), we can use the absolute magnitudes of Taurus objects to estimate a photometric distance for 2M2234+4041AB. The absolute J-band magnitudes of M5.5-M6.5 type objects in Taurus (Briceño et al. 2002; Luhman et al. 2003a; Luhman 2004b; Guieu et al. 2006) range from 4.57 to 7.39 mags with a mean of 6.51 mags. The absolute

J-band magnitudes include correction for extinction, exclude objects listed as binaries in the references above or discovered as binaries in Konopacky et al. (2007) and Kraus et al. (2006), and assume a distance to Taurus of 143 pc (Loinard et al. 2008). The dereddened J-band magnitude of 2M2234+4041A is 13.00 ± 0.30 mag (accounting for extinction uncertainties), implying a distance modulus of 6.49 and yielding a photometric distance of 199 pc. The range of absolute J-band magnitudes for Taurus objects corresponds to distance moduli of 5.61–8.43 mags, so distances of 132–484 pc for 2M2234+4041AB are plausible.

Given its young age (~ 1 Myr), null proper motion measurement and low radial velocity (Table 3), where could 2M2234+4041AB have originated? 2M2234+4041AB lies $1.5'$ from the well studied Herbig Ae/Be star, LkH α 233 (Calvet & Cohen 1978), and near the young K-type stars, LkH α 230, 231 and 232, and the B star, HD 213976 (Figure 10). Based on the geometry and temperature derived from observations of molecular gas (CO, NH $_3$, and H $_2$ CO) in the region, Olano, Walmsley & Wilson (1994) concluded that the LkH α stars likely formed from Condensation A of the LBN 437 complex, which is externally heated by HD 213976. HD 213976 has a *Hipparcos* measured parallax of 3.08 ± 0.56 mas (van Leeuwen 2007), corresponding to a distance of 325^{+72}_{-50} pc. If at this distance, the projected separation of 2M2234+4041AB is 51^{+11}_{-8} AU.

One method of establishing membership with a group of stars is common space motion. The null proper motion we measure for 2M2234+4041AB is consistent with the *Hipparcos* measured proper motion of HD 213976 (-1.67 ± 0.46 , -3.06 ± 0.45 mas/yr, van Leeuwen 2007). The proper motions reported by Ducourant et al. (2005) for LkH α 230 (4 ± 7 , -11 ± 3 mas/yr), LkH α 231 (-9 ± 5 , -8 ± 5 mas/yr), and LkH α 232 (-11 ± 5 , -3 ± 5 mas/yr) are also low. Our measured radial velocity of 2M2234+4041AB is -10.6 ± 0.5 km s $^{-1}$ (Table 3), which agrees with the radial velocity of LkH α 233 inferred from the relative velocities of its red and blue shifted jets (~ -10 km s $^{-1}$, Perrin & Graham 2007). The radial velocity of HD 213976 (-17.2 km s $^{-1}$) agrees with that of 2M2234+4041AB to within the ~ 10 km s $^{-1}$ spread observed for stars in the Taurus star-forming region (Bertout & Genova 2006). Kinetically, 2M2234+4041AB could be associated with the LkH α 233 group.

The distance typically assumed for the LkH α 233 group of young stars is 880 pc, a photometric distance of HD 213976 dating back to Herbig (1960). Photometric distances of 700 and 600 pc were found for LkH α 231 and 232 (Calvet & Cohen 1978), and Chernyshev & Shevchenko (1988) determined a photometric distance of 660 pc for 21 emission stars in the region. Given the large discrepancy between the astrometric distance (325^{+72}_{-50} pc) and the original photometric distance (880 pc) of HD 213976, it is worthwhile to re-examine the photometric distance to the LkH α 233 group and see if the discrepancy can be resolved.

Calculating a photometric distance for LkH α 233 is difficult due to the fact that its

circumstellar disk is viewed edge-on, and thus LkH α 233 is likely seen in scattered light (Perrin & Graham 2007). We can, however, obtain photometric distances for HD 213976, LkH α 232 and LkH α 231. Hernández et al. (2005) report an optical spectral type of B3 for HD 213976 and a low extinction ($A_V = 0.24 \pm 0.12$ mag). To obtain a photometric distance to HD 213976, we compare its brightness to B2–B4 type stars in Upper Scorpius. The mean absolute J-band brightnesses of twelve B2–B4 type Upper Scorpius members (Hernández et al. 2005) is -0.72 ± 0.73 mag (for $d = 145$ pc; de Zeeuw et al. 1999). By comparison to the brightness of Upper Scorpius objects, the 2MASS J-band magnitude of HD 213976 (7.19 ± 0.02 mag) implies a distance modulus of 7.91 mag and a distance of 382^{+153}_{-109} pc, in good agreement with the *Hipparcos* distance. Similarly, one can compare the brightnesses of LkH α 232 and LkH α 231 (SpTs of K3 and K4 respectively, Herbig & Bell 1988) to young Taurus objects of similar spectral type from Kenyon & Hartmann (1995). The mean absolute 2MASS J-band flux of K2–K5 type stars in Taurus (corrected for reddening using the published A_V 's of Kenyon & Hartmann (1995), and assuming a distance of 143 pc (Loinard et al. 2008)) is 3.80 ± 1.17 mag. Objects similar to Taurus K2–K5 stars at 325 pc should then have observed J-band magnitudes of 11.35 ± 1.17 , in good agreement with the 2MASS J-band photometry of LkH α 232 and 231 (11.18 ± 0.03 and 11.74 ± 0.02 mag respectively). Our newly calculated photometric distances of HD 213976, LkH α 232 and LkH α 231 are in good agreement with the astrometric distance of 325^{+72}_{-50} pc, which we adopt for the LkH α 233 group and 2M2234+4041AB. This distance is similar to the distance of Lacerta OB1 (368 ± 17 pc de Zeeuw et al. 1999), which lies ~ 5 degrees (~ 55 pc) away, and may indicate that the LkH α 233 group is a site of recent star-formation associated with Lac OB1.

3.5. Luminosity

To calculate the bolometric luminosities of 2M2234+4041A and B, we apply a bolometric correction (BC) to their extinction-corrected near-IR magnitudes. In theory, bolometric corrections can be made at any wavelength, but because 2M2234+4041A and B harbor circumstellar disks (§3.3.2 and 3.3.3), we choose to apply a bolometric correction at J-band (BC_J) to minimize possible contamination by circumstellar disk emission. To find an appropriate BC_J , we tabulated 2MASS J-band magnitudes and m_{bol} of field M5.5–M6.5 type dwarfs from Leggett et al. (2000). The mean BC_J is 2.00 mag with a standard deviation of 0.06 mag. For a distance of 325^{+72}_{-50} pc, and a solar M_{bol} of 4.76 mag, we calculate luminosities ($\log(L_*/L_\odot)$) of -0.27 ± 0.21 and -0.30 ± 0.21 dex for 2M2234+4041A and B, where the uncertainties were calculated from the uncertainties in A_V , distance, photometry, and BC_J .

3.6. Mass

Masses (and ages) of low-mass stars and brown dwarfs can be determined from evolutionary models by placing them on an H-R diagram with the objects’ luminosities determined photometrically and effective temperatures determined spectroscopically. The spectral type of 2M2234+4041AB, M6±1, corresponds to an effective temperature of 2990_{-110}^{+135} K according to the SpT- T_{eff} relationship appropriate for young objects of Luhman et al. (2003b). The top panel of Figure 11 shows the position of 2M2234+4041A on an H-R diagram with the evolutionary models of Baraffe et al. (1998) overlaid. 2M2234+4041A lies well above the 1 Myr old isochrone, making it difficult to estimate its mass using this method, though it is not uncommon for young objects to be overluminous relative to evolutionary models (e.g. Luhman 2004b).

Given the well established age of <5 Myr, we can estimate the mass of 2M2234+4041AB from evolutionary models using *age* and effective temperature. The bottom panel of Figure 11 shows the effective temperature and age range of 2M2234+4041AB, with iso-mass contours from Baraffe et al. (1998) overlaid. Fortunately, within the effective temperature range of 2M2234+4041AB, the iso-mass contours are nearly vertical, or age independent. At an age of 1–2 Myr, the T_{eff} of 2M2234+4041AB is closest to the 0.100 M_{\odot} iso-mass track, but masses of 0.060–0.175 M_{\odot} are also within the range of uncertainty in effective temperature and age. Though the possible mass of 2M2234+4041AB falls in a wide range, it is the first potential VLM member of the LkH α 233 group.

3.7. Orbital Period

We have measured the projected separation of 2M2234+4041AB to be 51_{-8}^{+11} AU, but the semimajor axis of the binary depends on its orbital parameters. Following the method of Torres (1999), we assume random viewing angles and a uniform eccentricity distribution between $0 < e < 1$ to derive a correction factor of $1.10_{-0.36}^{+0.91}$ (68.3% confidence limits) for converting the projected separation into a semimajor axis. This results in a semimajor axis of 57_{-21}^{+51} AU. For a total mass of 0.2 M_{\odot} , this corresponds to an orbital period of 1000_{-500}^{+1600} years. Unfortunately, the orbital period of 2M2234+4041AB is far too long for our observations to detect any significant relative motion of the binary.

3.8. Could 2M2234+4041AB be a Higher Order Multiple System?

As noted in §3.4 and shown in Figures 9 and 11, 2M2234+4041A is over-luminous relative to young Taurus M6 objects and the theoretical 1 Myr old isochrone. A common explanation for over-luminosity is unresolved multiplicity. Is it possible that 2M2234+4041AB is a higher order multiple system? Both components would need to have similar companions (i.e. a quadruple system) since the magnitudes and colors of 2M2234+4041A and B are nearly identical. We see no evidence of additional companions in three epochs of imaging (Table 1). Our LGS AO observations, however, would only be able to detect companions with separations $\gtrsim 13$ AU, whereas most field VLM binaries have tighter separations (Burgasser et al. 2007). Neither epoch of HIRES data show evidence of spectroscopic binarity, and the radial velocity shows no sign of variation. Interferometric or higher spatial resolution observations of the source would be needed to definitively rule out a higher order multiple system.

3.9. Will 2M2234+4041AB be Disrupted?

The 51 AU projected separation of 2M2234+4041AB is significantly wider than those typical of field VLM binaries (3–15 AU; Burgasser et al. 2007), which may indicate that binary systems similar to 2M2234+4041AB are disrupted before they reach the age of the field population (a few Gyr). In recent years, a handful of young, very wide (>100 AU) binaries have been discovered (Béjar et al. 2008; Bouy et al. 2006; Close et al. 2007; Luhman 2004a). Close et al. (2007) suggest that such young, wide systems might become unbound due to dynamical interactions with other young stars in their natal clusters. The separation and total mass of 2M2234+4041AB, however, meet the stability criteria of Close et al. (2007), meaning that systems similar to 2M2234+4041AB are likely to survive the dispersion of their cluster and are unlikely to be disrupted by encounters with field stars. Even if the actual masses of 2M2234+4041A and B were at the low-end of their possible mass range ($0.06 M_{\odot}$), the system would still be considered stable. The binding energy (GM_1M_2/a) of 2M2234+4041AB is $\sim 3.4 \times 10^{42}$ erg which is lower than all but two (out of 69) known field VLM binaries, indicating that systems similar to 2M2234+4041AB are rare, but possible among the field population.

4. Conclusions

As a part of our Keck LGS AO survey of young field objects, we discovered 2M2234+4041AB to be a binary. Over three epochs of imaging, the separation of the system does not change,

indicating that 2M2234+4041A and B are physically associated (though the low proper motion of the system makes it difficult to confirm if the pair is actually co-moving). The similarity in spectral shape and features as well as the fluxes and colors of 2M2234+4041A and B, suggest that both components have the same mass, spectral type, and age. From composite optical and near-IR spectroscopy, we derive a spectral type of M6 for the system. Evidence of the youth of the system is the detection of $K_S - L'$ excesses for 2M2234+4041A and B (presumably due to the presence of circumstellar disks). The level of excess, however, differs for the two components, indicating that the physical structures of their disks must be different. The strengths of H α and Br γ emission lines signify ongoing accretion, in agreement with the young (~ 1 Myr) age we derive for the system based on comparison of near-IR gravity sensitive spectral features with objects of similar spectral type and known age. By constraining the age and T_{eff} (from its spectral type), we determine individual masses of $0.10^{+0.075}_{-0.04}$ M_{\odot} for 2M2234+4041A and B by comparison to evolutionary models (Baraffe et al. 1998).

The original identification of 2M2234+4041AB was as a young, field object, not associated with any known star-forming regions (Cruz et al. 2003). However, 2M2234+4041AB lies 1.5' away from the well-studied HAeBe star, LkH α 233. LkH α 233 belongs to a small group of young stars (including LkH α 232, 231 and HD 213976), historically thought to lie at a distance of 880 pc (the photometric distance to HD213976; Herbig 1960). Recently, van Leeuwen (2007) reported a *Hipparcos* parallax measurement of 3.08 ± 0.56 mas for HD 213976, corresponding to a distance of 325^{+72}_{-50} pc. We re-examined the photometric distance to HD213976 as well as LkH α 231 and 232. Using the absolute J-band magnitudes of young objects (Taurus or Upper Scorpius), we derive photometric distances that are in agreement with the astrometric distance of 325 pc. 2M2234+4041AB is the first potential VLM member of the group. At a distance of 325 pc, the physical separation of 2M2234+4041AB is 51 AU. It is interesting that the first VLM object discovered in the region happens to be a young, wide binary. The binding energy of 2M2234+4041AB, indicates that it is unlikely to be dynamically disrupted (Close et al. 2007).

We gratefully acknowledge the Keck LGS AO team for their exceptional efforts in bringing the LGS AO system to fruition. It is a pleasure to thank Randy Campbell, Jim Lyke, Al Conrad, Hien Tran, Christine Melcher, Cindy Wilburn, Joel Aycock, Jason McElroy and the Keck Observatory staff for assistance with the observations. This work is based in part on data products produced at the TERAPIX data center located at the Institut d'Astrophysique de Paris. We also thank John Rayner and the IRTF Observatory staff for assistance with our SpeX observations and data reduction. We are appreciative of conversations with George Herbig on the origin of 2M2234+4041AB and the nature of other nearby young stars. We

also thank Jeffrey Rich for translating Chernyshev & Shevchenko (1988) into English. The authors sincerely thank Roy Gal for providing ‘Tek/UH88’ imaging of 2M2234+4041AB. We are grateful to Dan Jaffe, Casey Deen, Jasmina Marsh and Alan Tokunaga for providing the near-infrared spectrum of TWA8B. This research has benefitted from the M, L, and T dwarf compendium housed at DwarfArchives.org and maintained by Chris Gelino, Davy Kirkpatrick, and Adam Burgasser. KLC is supported by NASA through the Spitzer Space Telescope Fellowship Program, through a contract issued by the Jet Propulsion Laboratory, California Institute of Technology under a contract with National Aeronautics and Space Administration. MCL, KNA and TJD acknowledge support for this work from NSF grant AST-0507833 and AST-0407441. MCL also acknowledges support from an Alfred P. Sloan Research Fellowship. ES acknowledges support from NASA/GALEX grant NNX07AJ43G. KNA was partially supported by NASA Origins of Solar Systems grant NNX07AI83G.

REFERENCES

- Ahmic, M., Jayawardhana, R., Brandeker, A., Scholz, A., van Kerkwijk, M. H., Delgado-Donate, E., & Froebrich, D. 2007, *ApJ*, 671, 2074
- Allard, F., Hauschildt, P. H., Alexander, D. R., Tamanai, A., & Schweitzer, A. 2001, *ApJ*, 556, 357
- Allen, P. R. 2007, *ApJ*, 668, 492
- Allers, K. N., et al. 2007, *ApJ*, 657, 511
- Ardila, D., Martín, E., & Basri, G. 2000, *AJ*, 120, 479
- Baraffe, I., Chabrier, G., Allard, F., & Hauschildt, P. H. 1998, *A&A*, 337, 403
- Baraffe, I., Chabrier, G., Barman, T. S., Allard, F., & Hauschildt, P. H. 2003, *A&A*, 402, 701
- Barrado y Navascués, D., & Martín, E. L. 2003, *AJ*, 126, 2997
- Bate, M. R., & Bonnell, I. A. 2005, *MNRAS*, 356, 1201
- Béjar, V. J. S., Zapatero Osorio, M. R., Pérez-Garrido, A., Álvarez, C., Martín, E. L., Rebolo, R., Villó-Pérez, I., & Díaz-Sánchez, A. 2008, *ApJ*, 673, L185
- Bertin, E., & Arnouts, S. 1996, *A&AS*, 117, 393
- Bertout, C., & Genova, F. 2006, *A&A*, 460, 499

- Bonnell, I. A., Clark, P., & Bate, M. R. 2008, *MNRAS*, 389, 1556
- Bouy, H., Martín, E. L., Brandner, W., Zapatero-Osorio, M. R., Béjar, V. J. S., Schirmer, M., Huélamo, N., & Ghez, A. M. 2006, *A&A*, 451, 177
- Briceño, C., Luhman, K. L., Hartmann, L., Stauffer, J. R., & Kirkpatrick, J. D. 2002, *ApJ*, 580, 317
- Burgasser, A. J., Kirkpatrick, J. D., Cruz, K. L., Reid, I. N., Leggett, S. K., Liebert, J., Burrows, A., & Brown, M. E. 2006, *ApJS*, 166, 585
- Burgasser, A. J., Reid, I. N., Siegler, N., Close, L., Allen, P., Lowrance, P., & Gizis, J. 2007, *Protostars and Planets V*, 427
- Calvet, N., & Cohen, M. 1978, *MNRAS*, 182, 687
- Calvet, N., Muzerolle, J., Briceño, C., Hernández, J., Hartmann, L., Saucedo, J. L., & Gordon, K. D. 2004, *AJ*, 128, 1294
- Chabrier, G., Baraffe, I., Allard, F., & Hauschildt, P. 2000, *ApJ*, 542, 464
- Chabrier, G., Baraffe, I., & Plez, B. 1996, *ApJ*, 459, L91
- Chernyshev, A. V., & Shevchenko, V. S. 1988, *Astrofizika*, 29, 58
- Clarke, C. J., Gendrin, A., & Sotomayor, M. 2001, *MNRAS*, 328, 485
- Close, L. M., et al. 2007, *ApJ*, 660, 1492
- Cruz, K. L., et al. 2007, *AJ*, 133, 439
- Cruz, K. L., Reid, I. N., Liebert, J., Kirkpatrick, J. D., & Lowrance, P. J. 2003, *AJ*, 126, 2421
- Cushing, M. C., Rayner, J. T., & Vacca, W. D. 2005, *ApJ*, 623, 1115
- Cushing, M. C., Vacca, W. D., & Rayner, J. T. 2004, *PASP*, 116, 362
- Cutri, R. M., et al. 2003, *The IRSA 2MASS All-Sky Point Source Catalog*, NASA/IPAC Infrared Science Archive. <http://irsa.ipac.caltech.edu/applications/Gator/>
- D'Alessio, P., Calvet, N., Hartmann, L., Franco-Hernández, R., & Servín, H. 2006, *ApJ*, 638, 314

- de Zeeuw, P. T., Hoogerwerf, R., de Bruijne, J. H. J., Brown, A. G. A., & Blaauw, A. 1999, *AJ*, 117, 354
- Ducourant, C., Teixeira, R., Périé, J. P., Lecampion, J. F., Guibert, J., & Sartori, M. J. 2005, *A&A*, 438, 769
- Dupuy, T. J., Liu, M. C., & Ireland, M. J. *ApJ*, accepted
- Duquennoy, A., & Mayor, M. 1991, *A&A*, 248, 485
- Dullemond, C. P., Dominik, C., & Natta, A. 2001, *ApJ*, 560, 957
- Fitzgerald, M. P. 1968, *AJ*, 73, 983
- Fitzpatrick, E. L. 1999, *PASP*, 111, 63
- Ghez, A. M., et al. 2008, *ApJ*, 689, 1044
- Gizis, J. E. 2002, *ApJ*, 575, 484
- Goldman, B., Bouy, H., Zapatero Osorio, M. R., Stumpf, M. B., Brandner, W., & Henning, T. , *A&A*, accepted
- Gorlova, N. I., Meyer, M. R., Rieke, G. H., & Liebert, J. 2003, *ApJ*, 593, 1074
- Guieu, S., Dougados, C., Monin, J.-L., Magnier, E., & Martín, E. L. 2006, *A&A*, 446, 485
- Haisch, K. E., Jr., Lada, E. A., & Lada, C. J. 2001, *ApJ*, 553, L153
- Herbig, G. H. 1960, *ApJS*, 4, 337
- Herbig, G. H., & Bell, K. R. 1988, *Lick Observatory Bulletin*, Santa Cruz: Lick Observatory, 1988
- Hernández, J., Calvet, N., Briceño, C., Hartmann, L., & Berlind, P. 2004, *AJ*, 127, 1682
- Hernández, J., Calvet, N., Hartmann, L., Briceño, C., Sicilia-Aguilar, A., & Berlind, P. 2005, *AJ*, 129, 856
- Kenyon, S. J., & Hartmann, L. 1995, *ApJS*, 101, 117
- Kirkpatrick, J. D. 1992, Ph.D. Thesis,
- Kirkpatrick, J. D., et al. 2008, arXiv:0808.3153

- Kirkpatrick, J. D., Barman, T. S., Burgasser, A. J., McGovern, M. R., McLean, I. S., Tinney, C. G., & Lowrance, P. J. 2006, *ApJ*, 639, 1120
- Kirkpatrick, J. D., Henry, T. J., & McCarthy, D. W., Jr. 1991, *ApJS*, 77, 417
- Kirkpatrick, J. D., Henry, T. J., & Simons, D. A. 1995, *AJ*, 109, 797
- Krabbe, A., Gasaway, T., Song, I., Iserlohe, C., Weiss, J., Larkin, J. E., Barczys, M., & Lafreniere, D. 2004, *Proc. SPIE*, 5492, 1403
- Konopacky, Q. M., Ghez, A. M., Rice, E. L., & Duchêne, G. 2007, *ApJ*, 663, 394
- Kraus, A. L., White, R. J., & Hillenbrand, L. A. 2006, *ApJ*, 649, 306
- Larkin, J. E., et al. 2003, *Proc. SPIE*, 4841, 1600
- Leggett, S. K., Allard, F., Dahn, C., Hauschildt, P. H., Kerr, T. H., & Rayner, J. 2000, *ApJ*, 535, 965
- Leggett, S. K., et al. 2003, *MNRAS*, 345, 144
- Leggett, S. K., et al. 2002, *ApJ*, 564, 452
- Liu, M. C., Dupuy, T. J., & Ireland, M. J. *ApJ*, accepted
- Liu, M. C., Leggett, S. K., Golimowski, D. A., Chiu, K., Fan, X., Geballe, T. R., Schneider, D. P., & Brinkmann, J. 2006, *ApJ*, 647, 1393
- Liu, M. C., Najita, J., & Tokunaga, A. T. 2003, *ApJ*, 585, 372
- Liu, M. C. et al. *in preparation*
- Loinard, L., Torres, R. M., Mioduszewski, A. J., & Rodriguez, L. F. 2008, *ArXiv e-prints*, 804, arXiv:0804.4016
- Luhman, K. L. 2004, *ApJ*, 614, 398
- Luhman, K. L. 2004, *ApJ*, 617, 1216
- Luhman, K. L., Briceño, C., Stauffer, J. R., Hartmann, L., Barrado y Navascués, D., & Caldwell, N. 2003, *ApJ*, 590, 348
- Luhman, K. L., Stauffer, J. R., Muench, A. A., Rieke, G. H., Lada, E. A., Bouvier, J., & Lada, C. J. 2003, *ApJ*, 593, 1093

- McGovern, M. R., Kirkpatrick, J. D., McLean, I. S., Burgasser, A. J., Prato, L., & Lowrance, P. J. 2004, *ApJ*, 600, 1020
- McGroarty, F., Ray, T. P., & Bally, J. 2004, *A&A*, 415, 189
- Meynet, G., Mermilliod, J.-C., & Maeder, A. 1993, *A&AS*, 98, 477
- Mohanty, S., Jayawardhana, R., & Basri, G. 2005, *ApJ*, 626, 498
- Monet, D. G., et al. 2003, *AJ*, 125, 984
- Muzerolle, J., Hartmann, L., & Calvet, N. 1998, *AJ*, 116, 2965
- Muzerolle, J., Luhman, K. L., Briceño, C., Hartmann, L., & Calvet, N. 2005, *ApJ*, 625, 906
- Natta, A., Testi, L., Muzerolle, J., Randich, S., Comerón, F., & Persi, P. 2004, *A&A*, 424, 603
- Natta, A., Testi, L., & Randich, S. 2006, *A&A*, 452, 245
- Olano, C. A., Walmsley, C. M., & Wilson, T. L. 1994, *A&A*, 290, 235
- Padoan, P., & Nordlund, Å. 2004, *ApJ*, 617, 559
- Perrin, M. D., & Graham, J. R. 2007, *ApJ*, 670, 499
- Pravdo, S. H., Shaklan, S. B., Wiktorowicz, S. J., Kulkarni, S., Lloyd, J. P., Martinache, F., Tuthill, P. G., & Ireland, M. J. 2006, *ApJ*, 649, 389
- Preibisch, T., Brown, A. G. A., Bridges, T., Guenther, E., & Zinnecker, H. 2002, *AJ*, 124, 404
- Rayner, J. T., Toomey, D. W., Onaka, P. M., Denault, A. J., Stahlberger, W. E., Vacca, W. D., Cushing, M. C., & Wang, S. 2003, *PASP*, 115, 362
- Rebolo, R., Zapatero Osorio, M. R., Madruga, S., Bejar, V. J. S., Arribas, S., & Licandro, J. 1998, *Science*, 282, 1309
- Reid, I. N., & Cruz, K. L. 2002, *AJ*, 123, 466
- Reid, I. N., Lewitus, E., Allen, P. R., Cruz, K. L., & Burgasser, A. J. 2006, *AJ*, 132, 891
- Riaz, B., & Gizis, J. E. 2008, *ApJ*, 681, 1584
- Shkolnik, E., Liu, M. C., & Reid, I. N., 2009, *ApJ*, submitted

- Siegler, N., Close, L. M., Cruz, K. L., Martín, E. L., & Reid, I. N. 2005, *ApJ*, 621, 1023
- Simons, D. A., & Tokunaga, A. 2002, *PASP*, 114, 169
- Slesnick, C. L., Carpenter, J. M., & Hillenbrand, L. A. 2006, *AJ*, 131, 3016
- Stamatellos, D., & Whitworth, A. P. *MNRAS*, accepted
- Stauffer, J. R., Schultz, G., & Kirkpatrick, J. D. 1998, *ApJ*, 499, L199
- Tokunaga, A. T., Simons, D. A., & Vacca, W. D. 2002, *PASP*, 114, 180
- Torres, G. 1999, *PASP*, 111, 169
- Vacca, W. D., Cushing, M. C., & Rayner, J. T. 2003, *PASP*, 115, 389
- van Dam, M. A., et al. 2006, *PASP*, 118, 310
- van Leeuwen, F. 2007, *A&A*, 474, 653
- Webb, R. A., Zuckerman, B., Platais, I., Patience, J., White, R. J., Schwartz, M. J., & McCarthy, C. 1999, *ApJ*, 512, L63
- White, R. J., & Basri, G. 2003, *ApJ*, 582, 1109
- Whitworth, A., Bate, M. R., Nordlund, Å., Reipurth, B., & Zinnecker, H. 2007, *Protostars and Planets V*, 459
- Whitworth, A. P., & Zinnecker, H. 2004, *A&A*, 427, 299
- Wilson, R. E. 1953, *Carnegie Institute Washington D.C. Publication*, 0
- Wizinowich, P. L., et al. 2006, *PASP*, 118, 297

Table 1. Keck LGS AO Observations

Date (UT)	Filter ^a	Airmass	FWHM (mas)	Strehl ratio	Separation (mas)	Position angle (deg)	Δ mag
2006-Oct-14	K_S	1.50	78 ± 5	0.18 ± 0.02	158.5 ± 0.6	99.3 ± 0.3	0.05 ± 0.03
2007-Sep-06	J	1.08	37.2 ± 0.8	0.116 ± 0.005	158.2 ± 0.3	99.52 ± 0.09	0.06 ± 0.03
	H	1.07	40.8 ± 0.7	0.161 ± 0.008	158.5 ± 0.3	99.53 ± 0.15	0.096 ± 0.010
2008-Sep-08	L'	1.07	93 ± 3	0.58 ± 0.07	158.2 ± 1.0	100.1 ± 0.3	0.23 ± 0.03

^aAll photometry on the MKO system.

Note. — The tabulated uncertainties are the RMS of the measurements. The astrometric errors are computed by appropriately combining in quadrature: (1) the instrumental measurements from fitting the images of the binary (with errors derived from fitting of simulated binary images) and (2) the overall uncertainties in the NIRC2 pixel scale and orientation. See § 2.1 for details.

Table 2. Photometry of 2M2234+4041AB

Band	A+B (mag)	A ^a (mag)	B ^a (mag)
J	12.57 ± 0.02^b	13.29 ± 0.02	13.35 ± 0.03
H	11.83 ± 0.02^b	12.54 ± 0.02	12.63 ± 0.02
K_S	11.44 ± 0.02^b	12.17 ± 0.02	12.22 ± 0.03
L'	10.52 ± 0.06	11.16 ± 0.06	11.39 ± 0.06

^acalculated from composite photometry using Δ mag from Table 1

^bfrom the 2MASS All-Sky Point Source Catalog (Cutri et al. 2003)

Table 3. Properties of 2M2234+4041AB

Angular Separation ^a	$0.1582 \pm 0.0003''$
Position Angle ^a	$99.52 \pm 0.09^\circ$
Distance	325^{+72}_{-50} pc
Projected Separation ^b	51^{+11}_{-8} AU
Orbital Period	1000^{+1600}_{-500} yr
Proper Motion (mas yr ⁻¹)	$-1 \pm 6, 3 \pm 5$
Radial Velocity ^c (km s ⁻¹)	-10.6 ± 0.5

^avalues measured from the *J*-band image.

^bcalculated for a distance of 325^{+72}_{-50} pc

^cthe weighted mean of values in Table 4

Table 4. HIRES measurements of 2M2234+4041AB

Date (UT)	Li EW Å	H α EW Å	H α 10% width km s ⁻¹	Radial Velocity km s ⁻¹
2006 May 11	0.81 ± 0.03	-52.7 ± 0.1	314 ± 4	-10.37 ± 0.52
2006 Aug 12	0.84 ± 0.03	-39.2 ± 0.1	298 ± 4	-11.36 ± 0.95

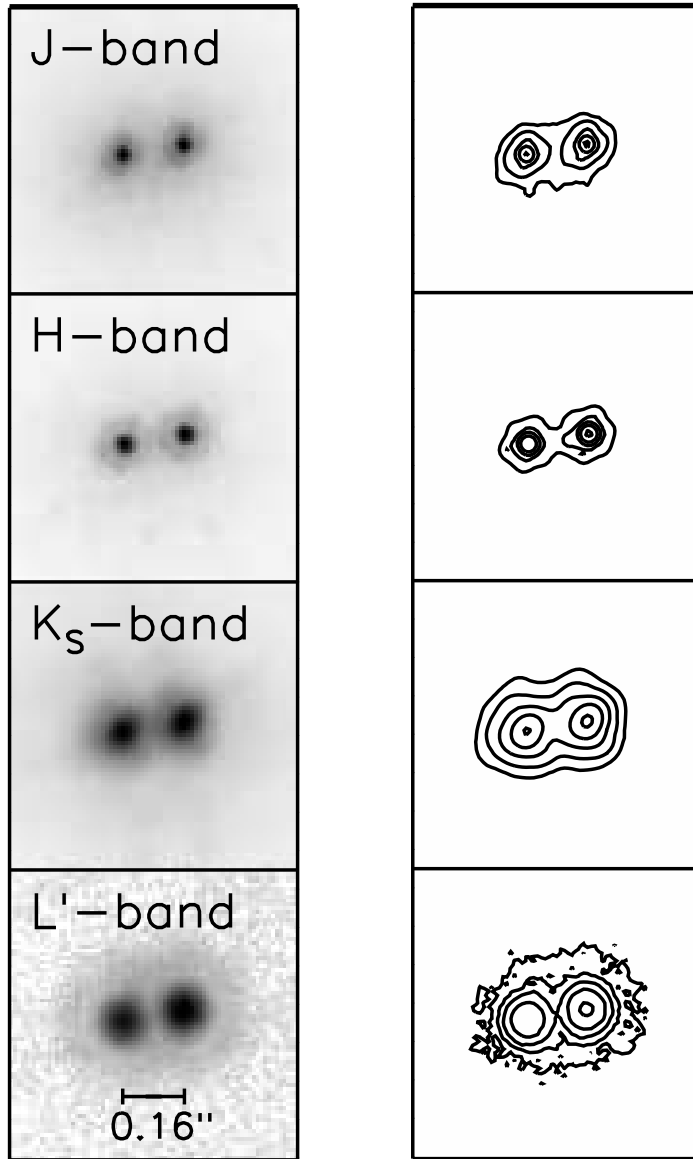


Fig. 1.— $JHK_S L'$ -band imaging of 2M2234+4041AB from Keck LGS AO. North is up and east is left. Each image is $0.75''$ on a side. The greyscale image uses a square-root intensity stretch. Contours are drawn from 90%, 45%, 22.5%, 11.2% and 5.6% of the peak value in each bandpass.

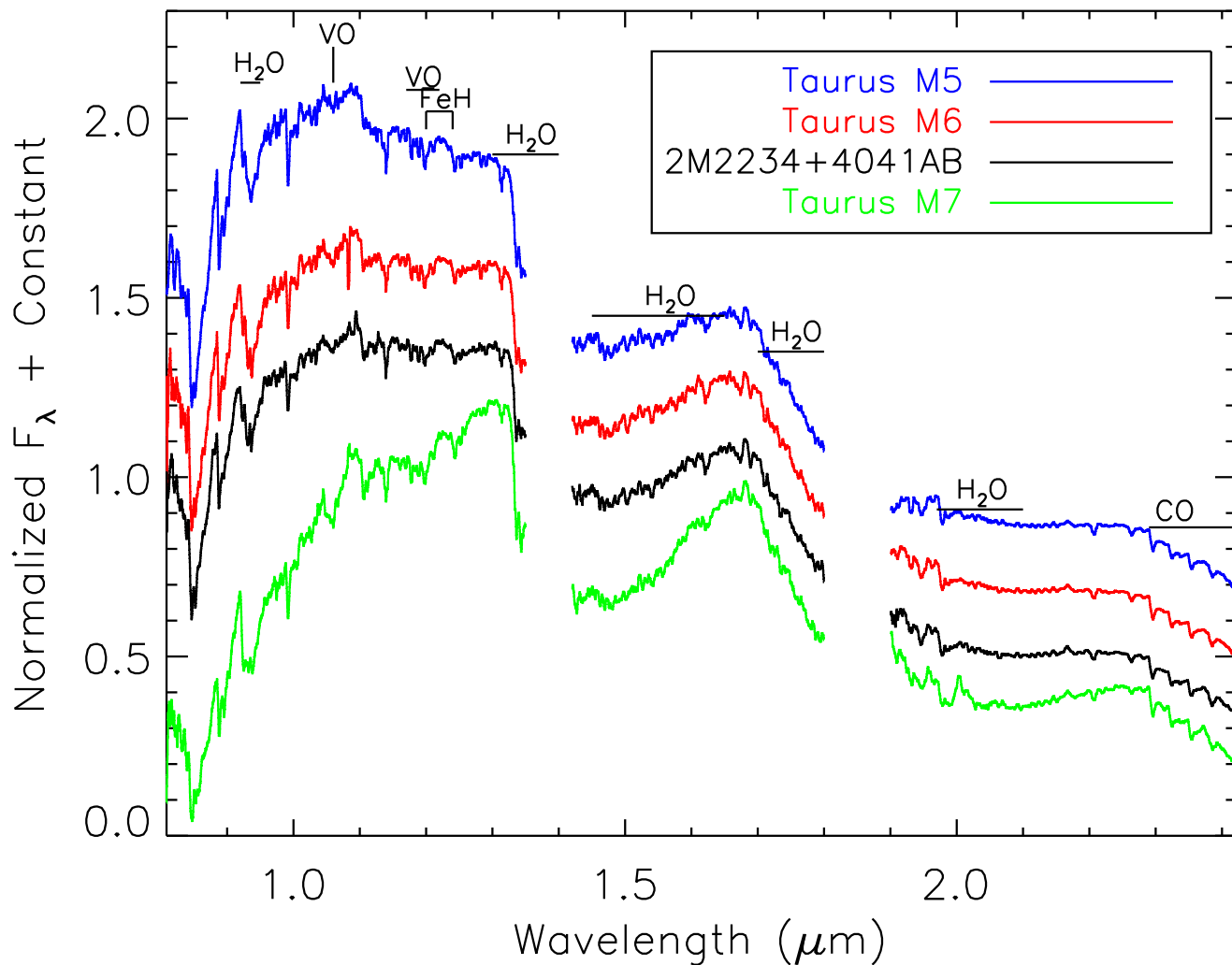


Fig. 2.— Composite SpeX spectrum of 2M2234+4041AB (black) compared to young Taurus objects with optical spectral types of M5 (Haro 6-32, blue), M6 (CFHT-BD-Tau 18, red), and M7 (CFHT-BD-Tau 4, green). The spectra of Taurus objects are smoothed to $\lambda/\Delta\lambda \sim 500$ and dereddened (using the reddening law of Fitzpatrick 1999) by A_V 's reported in Guieu et al. (2006) and Luhman (2004b). Spectral type sensitive features are labeled. The spectrum of 2M2234+4041AB (particularly its H₂O features) is best matched by a young Taurus M6.

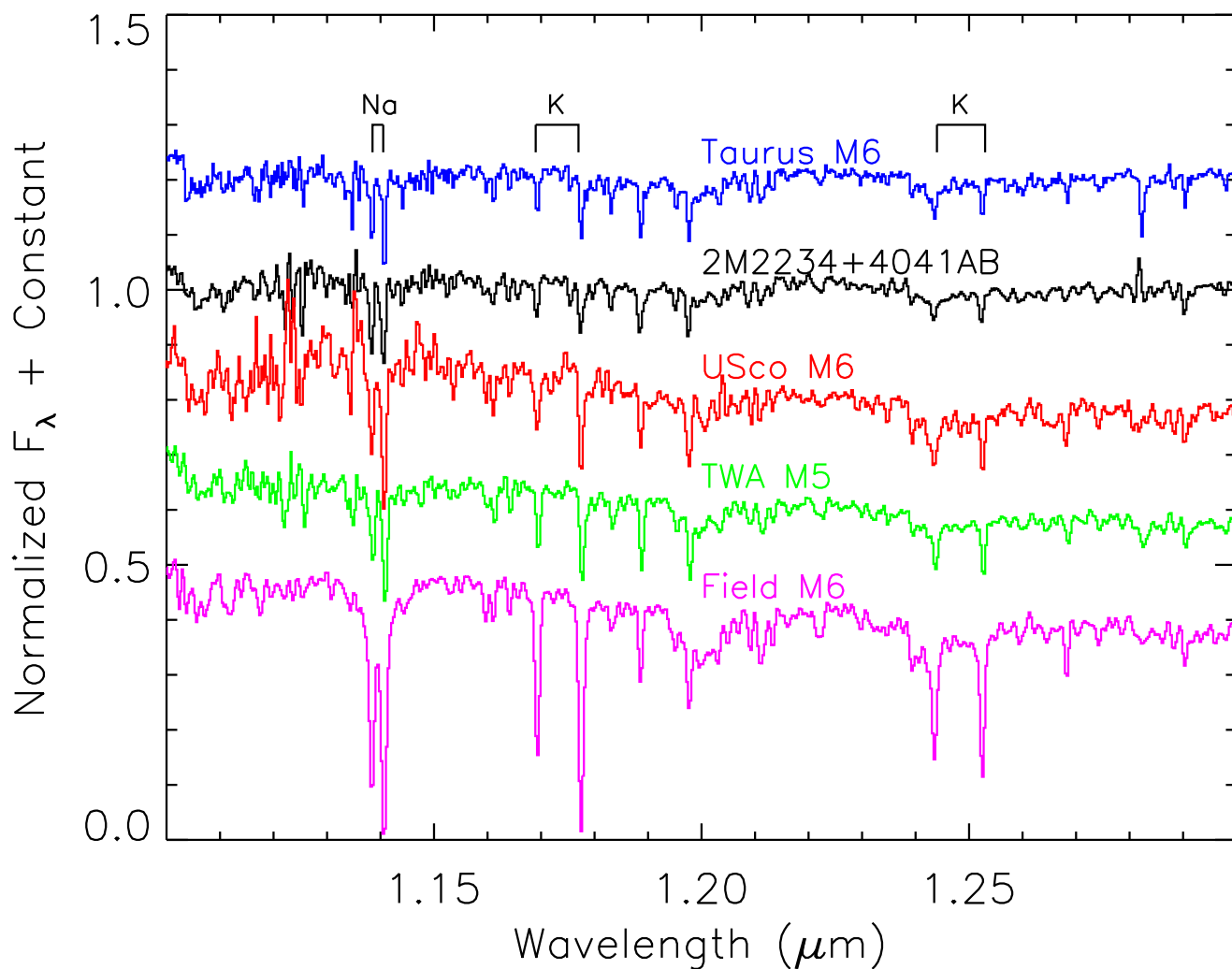


Fig. 3.— Integrated light J-band spectrum of 2M2234+4041AB (black) compared to a ~ 1 Myr old Taurus M6 (CFHT-BD-Tau 18, blue), a ~ 5 Myr old Upper Scorpius M6 (USco CTIO 75, red), a ~ 10 Myr old TWHydra M5 (TWA8B, green), and a ~ 1 Gyr field M6 (Gl406, magenta), all obtained with IRTF/Spex. Each spectrum is normalized by its median flux from 1.1–1.3 μm . The depths of the K I and Na I alkali lines (labeled) increase with age. The depths of the alkali lines in the spectrum of 2M2234+4041AB agree quite well with the line depths seen in the Taurus M6, implying an age of ~ 1 Myr for 2M2234+4041AB.

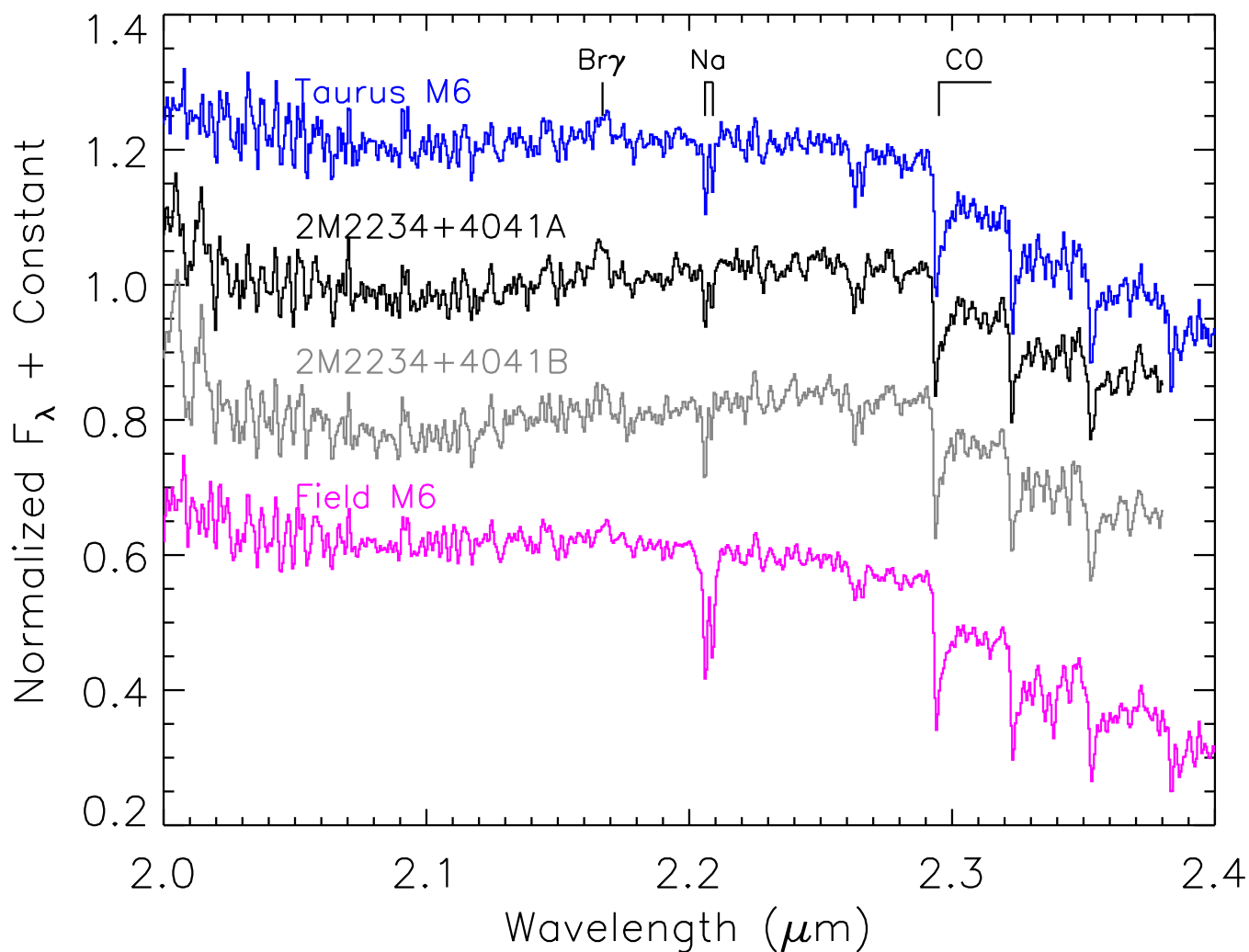


Fig. 4.— OSIRIS K-band spectra of 2M2234+4041A (black) and B (gray) compared to a ~ 1 Myr old Taurus M6 (CFHT-BD-Tau 18, blue) and a ~ 1 Gyr field M6 (Gl406, magenta). Each spectrum is normalized by its median from 2.0 to 2.4 μm . The 2.2 μm Na I alkali lines in components A and B are much weaker than for the field dwarf, indicating that both components are young. The continuum shape and 2.3 μm CO bandhead for components A and B are remarkably similar, in agreement with their identical spectral classification of M6.

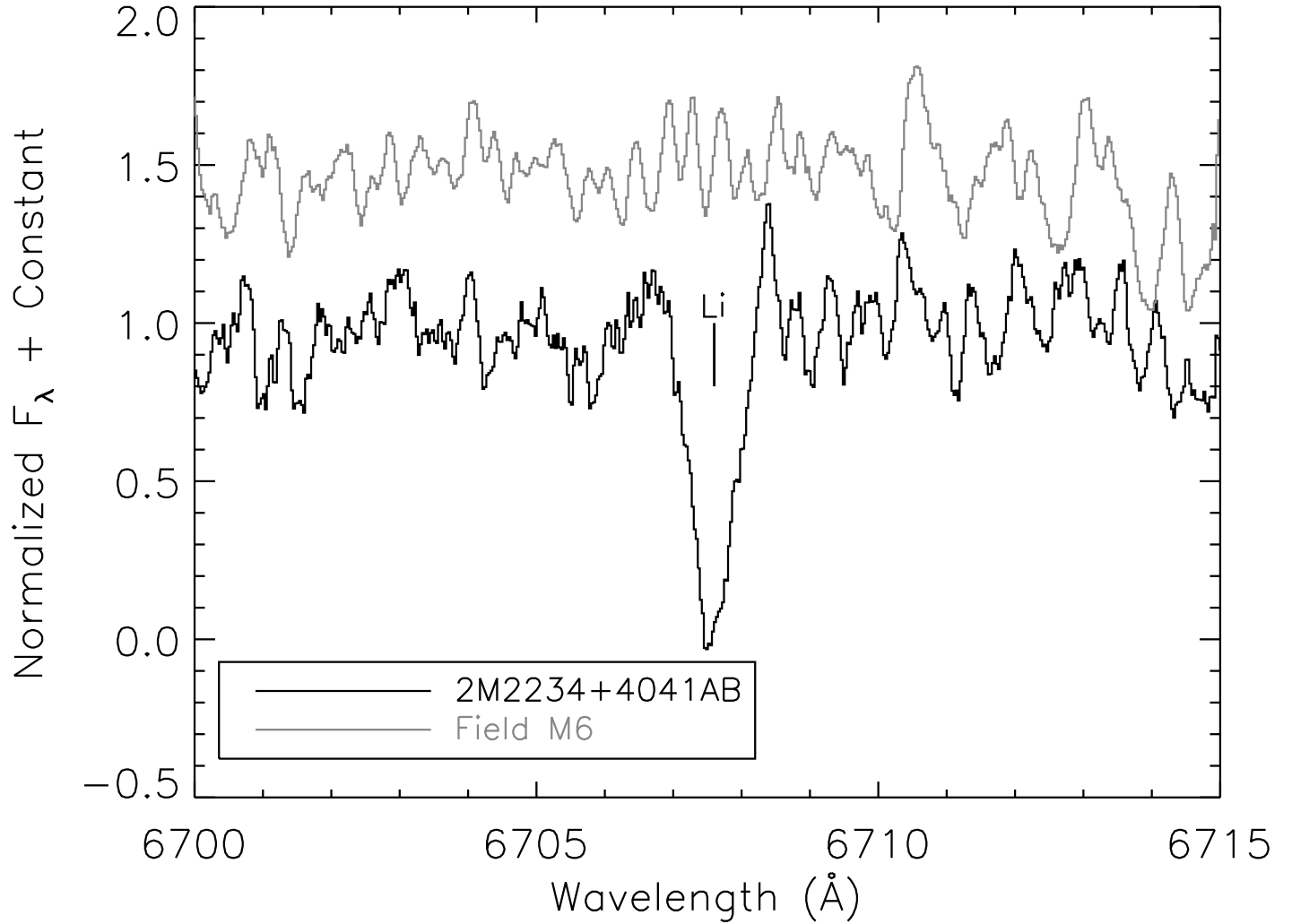


Fig. 5.— HRES spectrum of the lithium feature in 2M2234+4041AB compared with the M6 field dwarf NLTT 56194. The detection of lithium in the spectrum of 2M2234+4041AB indicates that it is younger than the Pleiades (~ 100 Myr).

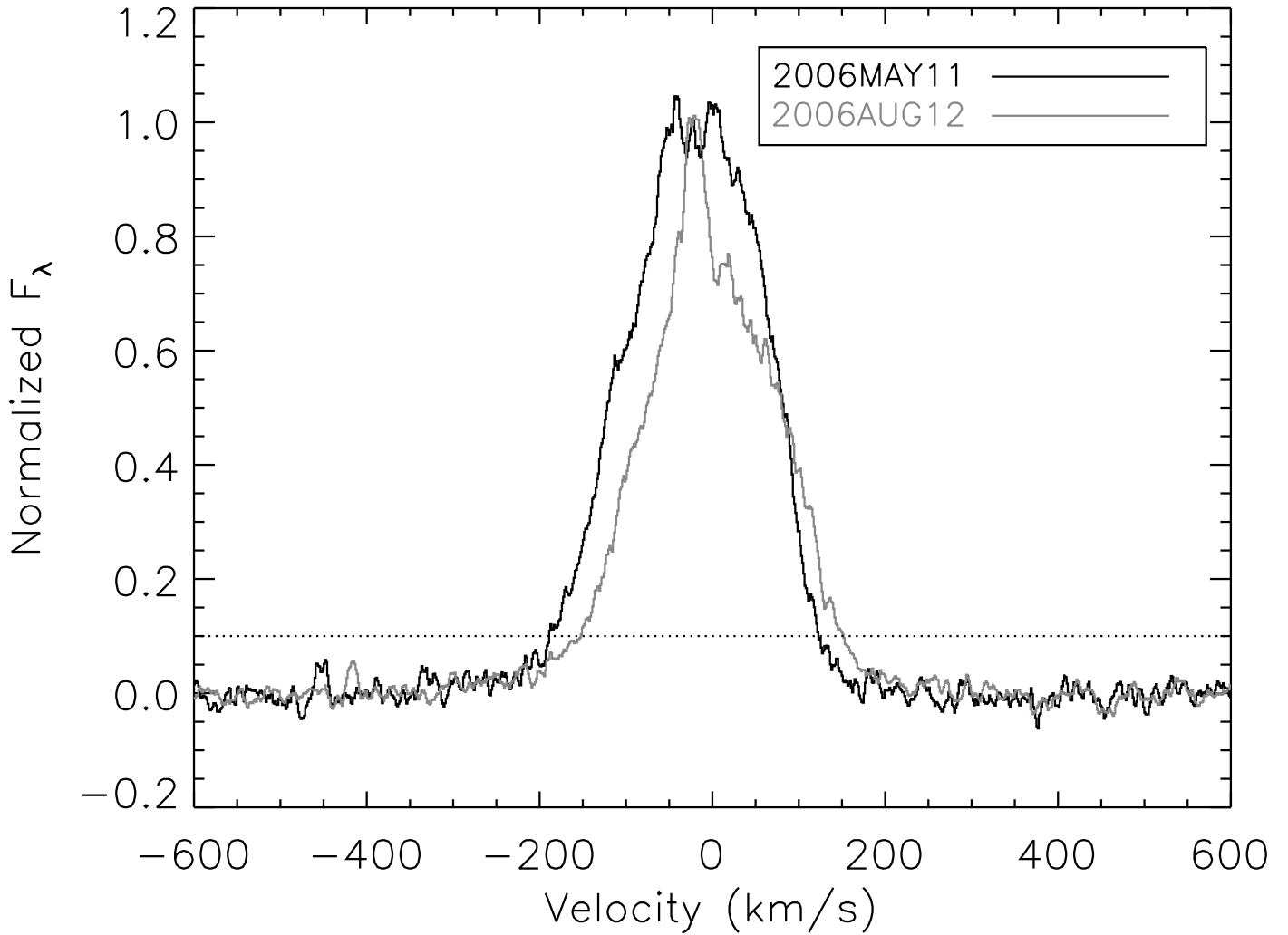


Fig. 6.— $H\alpha$ velocity profile of 2M2234+4041AB from Keck/HIRES observations on 2006 May 11 (black) and 2006 Aug 12 (gray). The profiles have been continuum-subtracted and normalized at the peak flux of the line. The dotted line shows the 10% flux level. The $H\alpha$ line equivalent widths and 10% widths imply ongoing mass accretion, and thus a young age for 2M2234+4041AB.

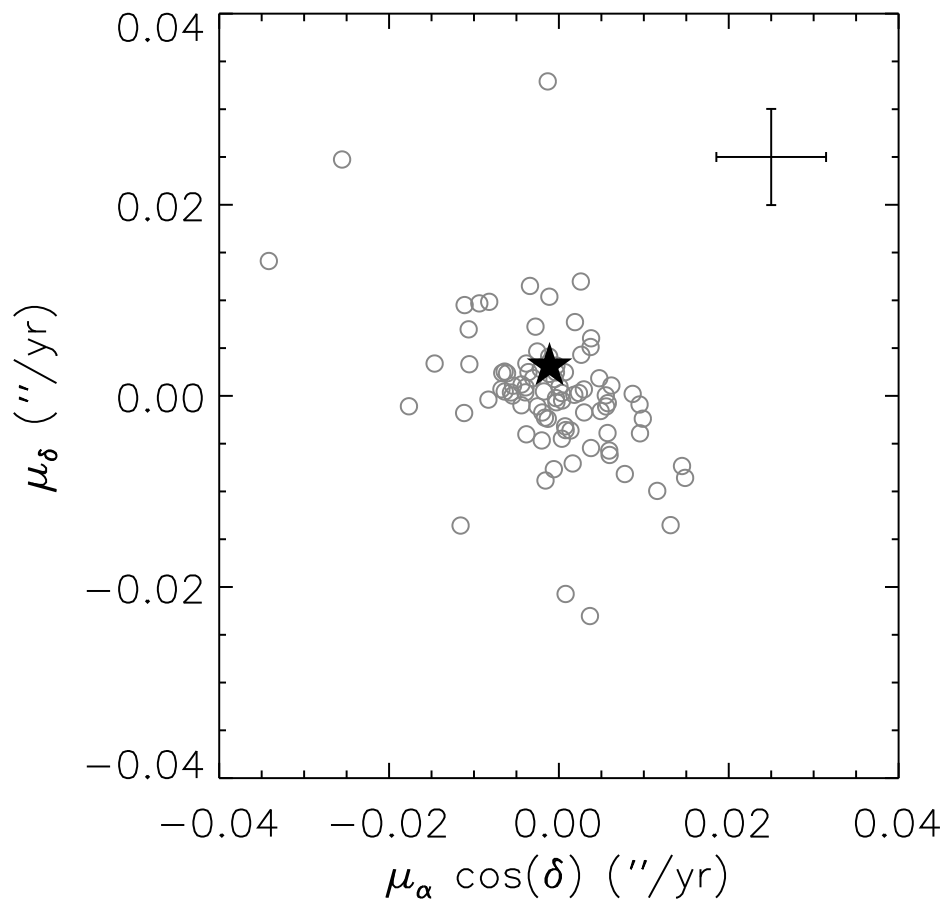


Fig. 7.— The proper motion of 2M2234+4041AB (filled star), as measured from POSS-I images (1952 July 20) and UH 2.2 m images (2007 July 31). The gray open circles show the proper motions measured for objects matched in the two epochs of images. The uncertainty (shown in the upper right) is the standard deviation found when transforming the POSS-I detected positions to the Tek image coordinates, divided by the time baseline.

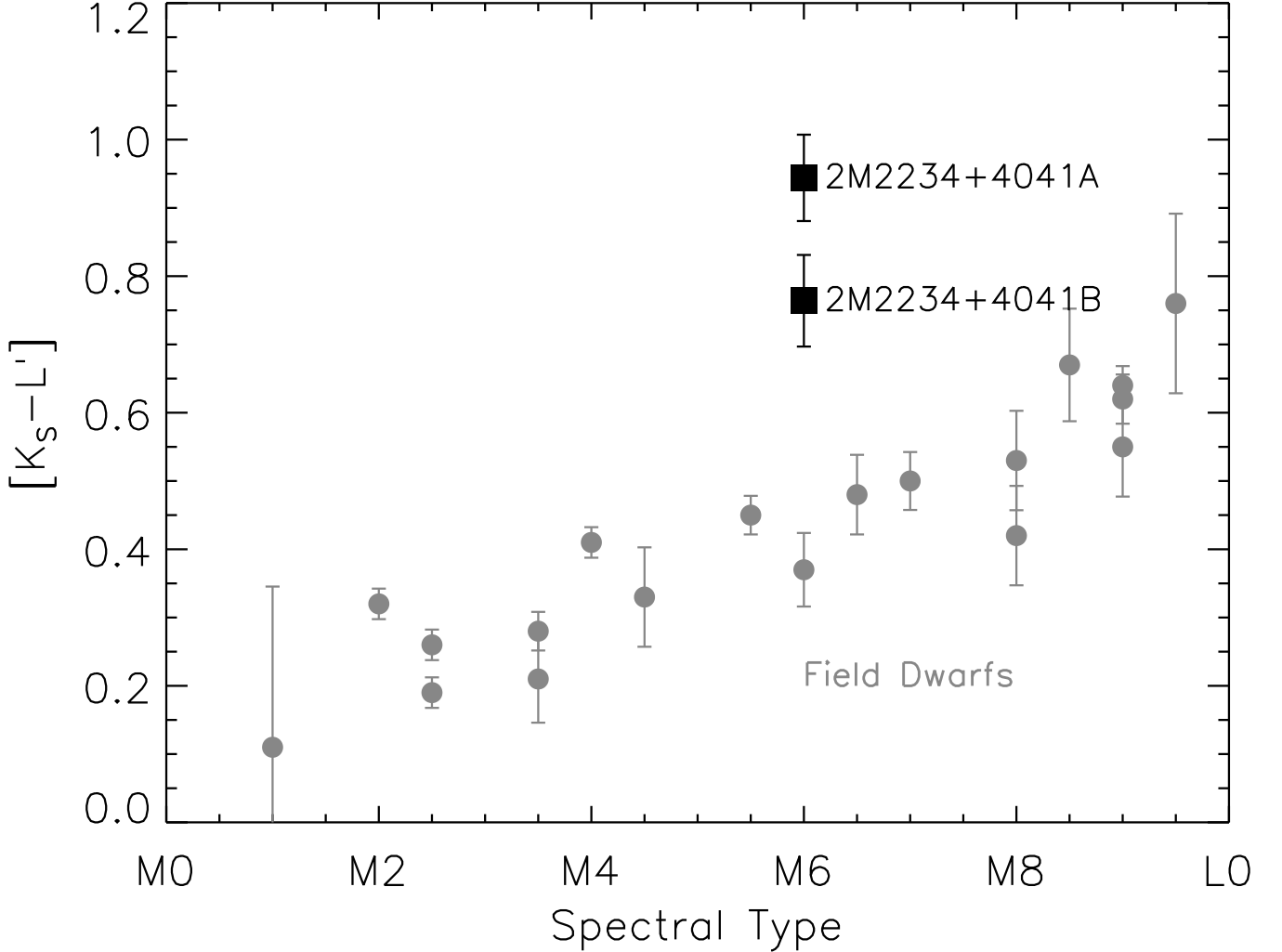


Fig. 8.— $K_S - L'$ colors of 2M2234+4041A and B compared to field dwarfs. The $K_S - L'$ colors of 2M2234+4041A and B have been corrected for reddening ($A_V=0.8$) using $(A_{K_S} - A_{L'})/A_V = 0.06$. The L' values for field dwarfs are from Leggett et al. (2002), Reid & Cruz (2002), and Leggett et al. (2003), and K_S is from 2MASS. The redder $K_S - L'$ colors of 2M2234+4041A and B, relative to field dwarfs of comparable spectral type, indicate that both components have infrared excesses, presumably due to the presence of circumstellar disks. The uncertainty in $K_S - L'$ for 2M2234+4041A and B is dominated by the L' calibration uncertainty. The relative difference in $K_S - L'$ color for the system, however, is known more precisely (0.18 ± 0.04 mag), indicating different physical structures for the two components' disks.

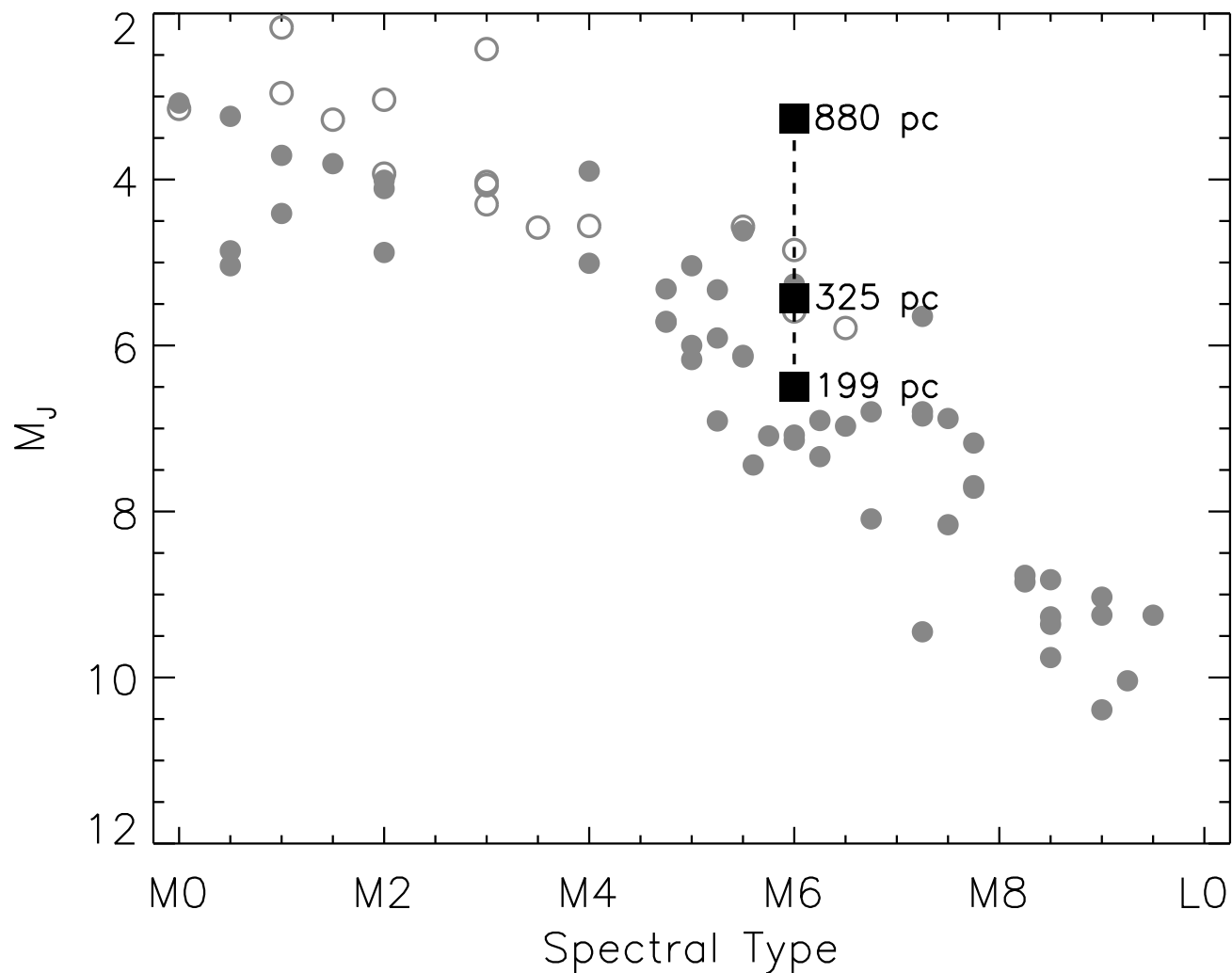


Fig. 9.— Spectral type vs. absolute J-band magnitude for 2M2234+4041A (black squares) and Taurus objects (gray circles, Briceño et al. 2002; Luhman et al. 2003a; Guieu et al. 2006). The open gray circles are objects listed as binaries in the references above, Kraus et al. (2006), or Konopacky et al. (2007). The black squares show the absolute J-band magnitude of 2M2234+4041A if it resides at: the distance typically assumed for LkH α 233 group (880 pc; Calvet & Cohen 1978), the Hipparcos distance to the nearby B3 star, HD213976 (325 pc; van Leeuwen 2007), and the photometric distance to 2M2234+4041A (calculated from the mean absolute J-band magnitude of M6 type Taurus objects). See §3.4 for details.

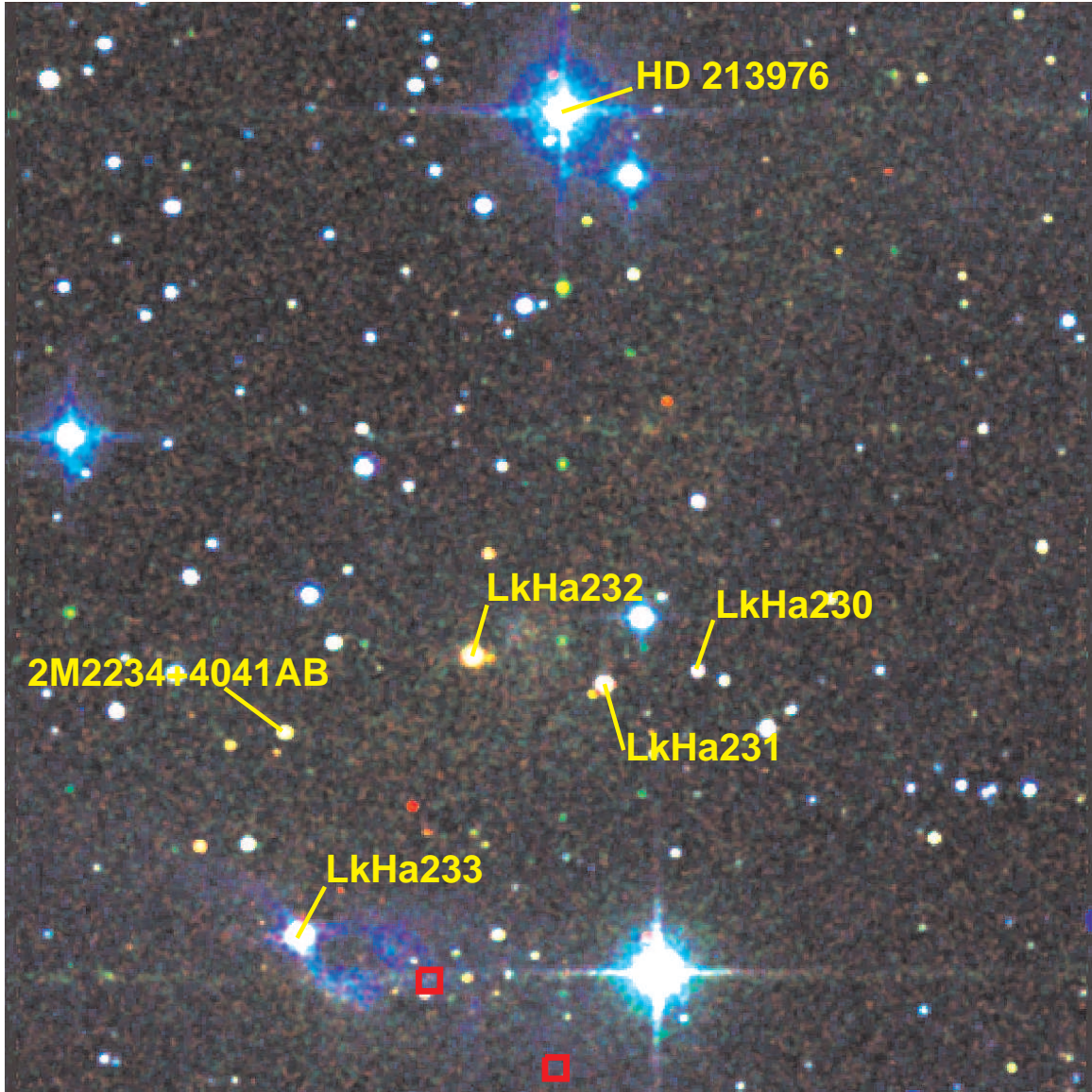


Fig. 10.— Three-color image showing the location of 2M2234+4041AB relative to other young stars in the region. The color mapping is red for 2MASS K_S -band, green for 2MASS J -band, and blue for POSS-I-Red images. Herbig-Haro objects from McGroarty, Ray, & Bally (2004) are displayed as red squares.

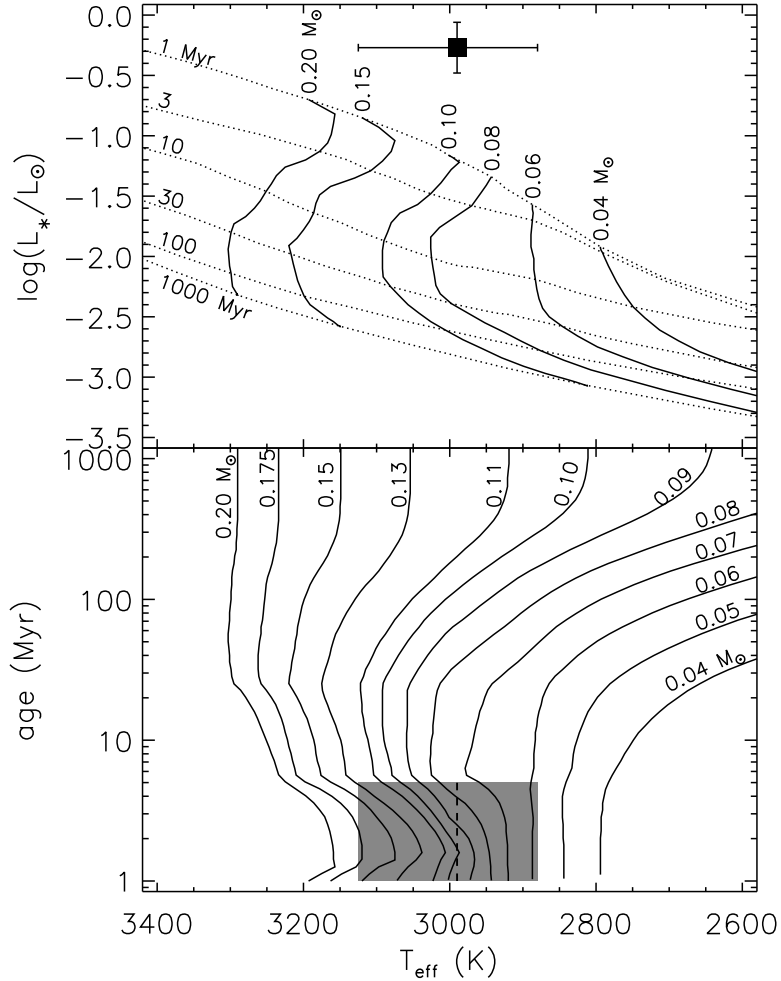


Fig. 11.— Mass determination for 2M2234+4041AB. Top: HR-diagram for 2M2234+4041A. Evolutionary models of Baraffe et al. (1998) are overlaid, with isochrones plotted as dotted lines and iso-mass contours plotted as solid lines. The square shows the position of 2M2234+4041A on this diagram, with the luminosity calculated in §3.5. The T_{eff} of 2M2234+4041AB is determined from its spectral type ($M6 \pm 1$) using the SpT- T_{eff} relation of Luhman et al. (2003b). 2M2234+4041A and B, having identical SpTs (and hence T_{eff} 's) and similar luminosities, are indistinguishable on this diagram. 2M2234+4041A is more luminous than the youngest isochrone in this diagram, making a mass estimate difficult. Bottom: Effective temperature vs. age diagram. Iso-mass contours are from the evolutionary models of Baraffe et al. (1998). The T_{eff} of 2M2234+4041AB is displayed as a dashed line, and the shaded region shows the likely age and T_{eff} range of 2M2234+4041AB. The age range (< 5 Myr) is based on the presence of a circumstellar disk, evidence of accretion, and the strength of the K I and Na I lines (see §3.3 for details). Fortunately, the iso-mass contours at young ages are nearly vertical (age insensitive). Thus, we determine a mass for 2M2234+4041A and B of $0.100 M_{\odot}$, but masses of 0.060 – $0.175 M_{\odot}$, are possible.